A Survey of Positioning Systems Using Visible LED Lights

Yuan Zhuang, *Member, IEEE*, Luchi Hua, Longning Qi, Jun Yang, Pan Cao, *Member, IEEE*, Yue Cao, *Member, IEEE*, Yongpeng Wu, *Senior Member, IEEE*, John Thompson, *Fellow, IEEE*, and Harald Haas, *Fellow, IEEE*

***Abstract*—As Global Positioning System (GPS) cannot provide satisfying performance in indoor environments, indoor positioning technology, which utilizes indoor wireless signals instead of GPS signals, has grown rapidly in recent years. Meanwhile, visible light communication (VLC) using light devices such as light emitting diodes (LEDs) has been deemed to be a promising candidate in the heterogeneous wireless networks that may collaborate with radio frequencies (RF) wireless networks. In particular, light-fidelity has a great potential for deployment in future indoor environments because of its high throughput and security advantages. This paper provides a comprehensive study of a novel positioning technology based on visible white LED lights, which has attracted much attention from both academia and industry. The essential characteristics and principles of this system are deeply discussed, and relevant positioning algorithms and designs are classified and elaborated. This paper undertakes a thorough investigation into current LED-based indoor positioning systems and compares their performance through many aspects, such as test environment, accuracy, and cost. It presents indoor hybrid positioning systems among VLC and other systems (e.g., inertial sensors and RF systems). We also review and classify outdoor VLC positioning applications for the first time. Finally, this paper surveys major advances as well as open issues, challenges, and future research directions in VLC positioning systems.**

***Index Terms*—LED, visible light communication (VLC), indoor positioning, outdoor positioning, hybrid positioning, localization.**

I. Introduction

POSITIONING systems used for the purpose of estimating user location are the basis for navigation-based services. As the present mainstream in positioning systems, Global Positioning System (GPS) is widely used in aircraft, vehicles, and portable devices in order to provide real-time positioning and navigation [1]. However, in challenging environments, such as urban canyons and indoors, GPS positioning and navigation is inaccurate and discontinuous since the signals transmitted by satellites are usually degraded and interrupted by clouds, ceilings, walls, and other obstructions [2], [3]. A hot topic in the positioning service is the "last meter" problem, in that indoor applications require much more accurate positioning than outdoor applications. Consequently, indoor positioning systems (IPS) using indoor wireless signals (e.g., WiFi [4], [5], Bluetooth [6], [7], radio frequency identification (RFID) [8], [9], and ZigBee [10]) have been proposed to fill the gap of GPS signals to improve the performance of indoor positioning. Over the last few decades, these signals have been employed in IPS technologies, among which WiFi and Bluetooth positioning systems are mostly utilized and which have already been widely deployed in current smart devices.

Positioning systems based on light emitting diodes (LEDs) emerged in recent years, which leverages visible light signal instead of radio frequency (RF). Before that, LED was known for its promising application in the communication field, namely visible light communication (VLC) [11]. The key to these applications is that LED has many important features. These features are:

i) high bandwidth (100's of MHz) [12] for safe, secure, and high speed wireless data transmission. The sampling rate of current photo detectors can easily be up to tens of MHz [12]. Unlike other wireless signal positioning technologies, VLC systems in different rooms are independent and they do not interfere with each other since light cannot penetrate opaque obstructions, which enables more secure wireless communication.

ii) "green" technology. A LED consumes low power (100 mW for 10-100 Mbps) and is quite energy-efficient. Besides, LEDs do not generate electromagnetic or radio interference [13].

iii) long lifetime. LEDs can keep functioning for up to 10 years with reliable illumination [13].

iv) cost-efficient [14]. Reliable LEDs and photo detectors cost less than $1 [13]. Along with the advantage of a long lifetime and energy efficiency, maintenance fees are also low.

Therefore, it is predictable that implementing a novel localization technology based on VLC systems has a great

Manuscript received January 5, 2017; revised October 5, 2017 and December 12, 2017; accepted January 28, 2018. Date of publication February 15, 2018; date of current version August 21, 2018. This work was supported by the National Science Foundation of China under Grant 61474022. *(Corresponding author: Jun Yang.)*

Y. Zhuang, L. Hua, L. Qi, and J. Yang are with the National ASIC Center, Southeast University, Nanjing 210096, China (e-mail: zhy.0908@gmail.com; hualuchi@gmail.com; longn_qi@seu.edu.cn; dragon@seu.edu.cn).

P. Cao is with the School of Engineering and Technology, University of Hertfordshire, Herts AL10 9AB, U.K. (e-mail: p.cao@herts.ac.uk).

Y. Cao is with the Department of Computer and Information Sciences, Northumbria University, Newcastle upon Tyne NE1 8ST, U.K. (e-mail: yue.cao@northumbria.ac.uk).

Y. Wu is with the Department of Electronic Engineering, Shanghai Jiao Tong University, Minhang 200240, China (e-mail: yongpeng.wu@sjtu.edu.cn).

J. Thompson and H. Haas are with the School of Engineering, University of Edinburgh, Edinburgh EH9 3JL, U.K. (e-mail: john.thompson@ed.ac.uk; h.haas@ed.ac.uk).

Digital Object Identifier 10.1109/COMST.2018.2806558

TABLE I
COMPARISON OF PREVIOUS WORKS WITH OURS

Features	[23]	[15]	[24]	[25]	Ours
Application Scenarios	NO	YES	NO	YES	YES
Channel Model	NO	General	General	NO	Explicit
Multiplexing Protocols	NO	General	General	Mentioned	Explicit
Field of View	NO	NO	General	NO	Explicit
Noise	NO	Mentioned	General	NO	Explicit
Multipath Effect	NO	NO	Mentioned	General	Explicit
Error	General	NO	General	NO	Explicit
Trilateration	General	General	General	NO	Explicit
Fingerprinting	General	General	General	NO	Explicit
Proximity	General	NO	General	Explicit	General
Multilateration	General	General	General	NO	Explicit
Triangulation	General	General	General	Explicit	Explicit
Image Transformation	NO	Explicit	General	NO	General
Advanced Filters	NO	NO	Mentioned	General	Explicit
Angular Diversity Approach	NO	NO	NO	YES	YES
Rolling Shutter Effect	NO	NO	Mentioned	NO	Explicit
Double Camera Approach	NO	YES	YES	YES	YES
Hybrid Positioning System	NO	NO	General	General	Explicit
Outdoor Positioning System	NO	NO	Mentioned	NO	YES
Performance Analysis	General	General	General	Explicit	Explicit
Performance Comparison	YES	YES	YES	YES	YES

potential, which has encouraged both academia and industry to step into the field. Over the past few years, many algorithms for LED-based positioning have been proposed and verified by experiments. Positioning systems using LEDs have shown to be more accurate (0.1-0.35 m positioning error) when compared to WiFi (1-7 m), Bluetooth (2-5 m), and other technologies [15]. Furthermore, some systems have achieved millimeter-level positioning accuracy [16]–[18]. In 2007, Japan Electronics and Information Technology Industries Association (JEITA) proposed standardizing transmission identification signals from LEDs to the communication concept of visible light beacon [19], [20]. Published in 2011, IEEE 802.15.7 was a standard that defined the physical layers for short-range visible light communications in which flicker mitigation and dimming support were integrated and focused on [21].

During recent years, many in-depth surveys on VLC have been published [12]–[14], [22]. For instance, the research [14] studied system design, various VLC characteristics, channel properties, and medium access techniques. In addition, various VLC applications including indoor positioning were mentioned. The work [13] surveyed smart lighting and free-space-optical communication based on mobile phones. The survey [22] studied the theoretical limitations of outdoor free-space-optical channels and discussed relevant research that provide approaches, such as diversity techniques and adaptive transmission, to overcome these limitations. The work [12] offered a comprehensive survey of VLC systems as well as methods to improve their performance, and focused on the main challenges in indoor applications. All of these surveys, however, did not focus on indoor VLC localization techniques although a general concept was mentioned in [14].

The literature that relates to VLC positioning systems was examined in [15] and [23]–[25]. The work [23] proposed three positioning algorithms and compared their performances. The survey [15] provided a comprehensive study on positioning systems and algorithms and classified positioning systems into photodiode-based systems and camera-based systems. In the article [24], an intensive effort was made to present the published literature of VLC positioning systems. Various positioning algorithms were presented and linked to related works. The survey [25] proposed a taxonomy based on the used positioning methods and focused on the accuracy of IPSs in literature. A comparison of these surveys, including our work, is shown in TABLE I. The article [23], which was published in 2013, only generally discussed positioning algorithms. Features of VLC positioning systems such as channel and multiplexing protocols were not discussed. In the survey [15], proximity methods and filter techniques were not included and neither were key techniques relating to camera-based positioning, such as the rolling shutter effect. The work [24] focused on the positioning algorithms while many characteristics of the VLC positioning (e.g., multiplexing protocols, field of view, and rolling shutter effect) were only generally discussed or mentioned. In addition, this article did not discuss either the application scenarios of VLC positioning or specific positioning approaches, such as the angular diversity approach. In the work [25], channel model, noise, and error were not discussed. Moreover, positioning methods such as trilateration, fingerprinting, and multilateration were not included.

Different from former surveys, we classify VLC positioning systems with respect to the type of receiver and the number of LED sources, which helps distinguish the application scenario for each design. Researches on outdoor LED positioning are also studied to make this article more comprehensive, which is another important feature of our work. The parameter "field of view" is deeply investigated and a clear distinction is made between a photodiode-based system and a camera-based system. Discussion on the advanced filters including Kalman filter (KF) and particle filter (PF) are also presented in this survey. For camera-based IPS, rolling shutter effect is explicitly discussed to show how it is applied to get identification information of LEDs. Another difference from [15] and [24] is that the discussion of all the key features of the VLC positioning

system are tightly connected with the positioning system (i.e., channel model, multiplexing protocols, field of view, noise, multipath, and error). For example, in the discussion of channel model, we explain Lambertian orders for both LED and receiver, illustrate how to determine these parameters for practical experiments, and show the influence of these parameters on the whole systems. Positioning algorithms all come with explicit explanation on the application in VLC positioning, as well as the presentation of experiment results.

In this article, we shall systematically introduce and explain the complete positioning system based on visible LED lights, and also provide a brief survey of the relevant works as a tutorial for interested readers. This article has categorized all the algorithms in the surveyed works into several main positioning methods. In particular, the article will emphasize those mutual problems that may occur in LED-based IPSs. Some advice is also offered for future work. The remainder of this article will be organized as follows: in Section II, an overview of an LED-based indoor positioning system will be presented; in Section III, the essential characteristics of the system will be discussed; in Section IV, this article will classify the previous positioning algorithms based on received optical signals, namely time of arrival (TOA)/time difference of arrival (TDOA), received signal strength (RSS), and angle of arrival (AOA), and present advanced filtering algorithms operated in positioning systems; in Section V, this article will emphasize specific hardware configuration for an LED positioning system. This article presents and categorizes the current LED-based indoor positioning systems into photodiode-based (PD-based) system, camera-based system, hybrid system, and outdoor system; in Section VI, this article will evaluate and compares these IPSs using metrics including accuracy, complexities, costs, limitations, and commercial availability; in Section VII, we will discuss challenges and future directions for research and implementation; finally, in Section VIII, we will summarize our work.

II. Overview

A. Applications

During the past few years, indoor positioning systems based on WiFi and Bluetooth have been deployed commercially while most LED-based IPS applications are still under development and subject to field trials. From 2015, some enterprises began to commercialize LED positioning systems and in that year Carrefour in Lille, France, piloted Philips' intelligent lighting devices to help customers find products of interest and also to track relevant discount information [26]. Meanwhile, Bytelight, which was acquired by Acuity Brands in 2015, has created professional indoor positioning system solutions based on LED lights since 2011 [27]. In April 2016, Qualcomm released its own LED guiding system – Lumicast – which achieved centimeter-level positioning accuracy for indoor venues [28]. In general, LED-based IPS technology can be deployed in the following discussed scenarios.

1) Indoor Public Spaces: such as stadia, theatres, opera houses, museums and exhibition centers where people might easily get lost, location-aware services would be a valuable asset for guiding them to their seats, toilets and elevators [29]. IPS can also inform visitors about exhibits around their locations and navigate people to their areas of interest. Moreover, IPS will help staff to control visitor traffic and improve visitor flow if a particular section becomes congested. Since these public spaces have already been equipped with illumination, LED localization systems can be easily implemented with little additional equipment.

2) Factories and Logistics: IPS enables factories and logistics centers to locate employees and assets efficiently in order to improve security and management [30]. It can also be used to navigate robots and manage inventory storage. Furthermore, IPS enables to locate processing units and monitor products. This will provide flexibility for reconfiguration and rezoning for changing mandates and needs, contributing to energy and maintenance savings, as well as operational efficiency.

3) Shopping Centers: IPS is particularly meaningful for complex floorplans where stores and facilities are scattered throughout a building, since navigational services will provide efficient directions to visitors. It will also benefit merchants, firstly, since they can deliver their advertisements and coupons to potential customers as they enter the mall and, secondly, it can promote personalized shopping experiences by offering advices regarding brands and price comparisons when a "tracked" customer approaches a brand counter, and thirdly, customer purchase behavior can be recorded to highlight sales hotspots to enable them to optimize their shelf layouts.

4) Airports and Train Stations: IPS location-aware services can assist passengers to reach their boarding points, find correct routes, train or bus exits, booking offices, restrooms, toilets and stores. This is especially useful information for foreign and first time visitors. Similarly, the managers of airports or railway stations can locate passengers, control traffic and manage luggage, etc.

5) Healthcare Facilities: Many hospitals already have many LED illuminations installed. Therefore, the cost of transmitters can be saved to provide location service. The positioning service in hospital can track wheelchairs and medical devices and also to make emergency services more accessible. Patients with impaired vision or other handicaps can also benefit from this system – for example, an LED device attached to a wheelchair will find its way, unaided, to the nearest elevator. To achieve this goal, the device receives signals from the ceiling lights, estimates the patient's coordinates, gives directions to the destination and warns of any obstacles.

6) Other Fields: LED signals can replace GPS for high-accuracy outdoor navigation by using a combination of existing traffic lights and auxiliary LED beacons [31]. An LED-based IPS system was explored to enhance VLC system, where transmission performance was improved to 410Mb/s [32]. This application needed millimeter-level accuracy to calibrate the incidence angle to below 1°. Overall, it is challenging to design an appropriate system that works for a particular target or environment.

B. IPS Architecture

LED-based IPS shares the same architecture with other technologies such as WiFi-based and Bluetooth-based

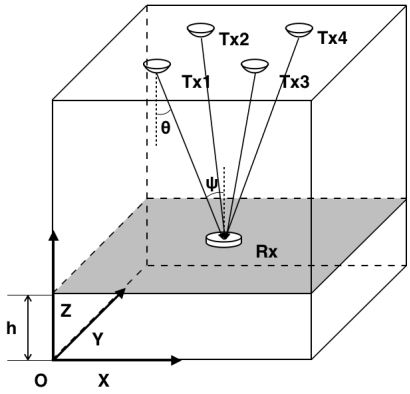

Fig. 1. A typical prototype of an LED-based indoor positioning system.

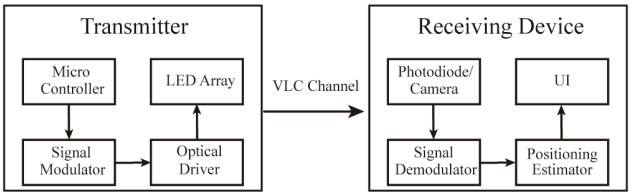

Fig. 2. General architecture for a simplex VLC positioning system.

systems [15]. We assume an indoor environment – an office, a supermarket, or a hallway – as a cube-shaped space, and illustrate a typical prototype of the system in Figure 1 where several LEDs (transmitters) are deployed on the ceiling as basic illumination. An optical sensor, which in this article refers to a photodiode or a camera, is placed at h [m] in height above the ground and used as a receiver. Usually, the optical sources (Tx1∼4) transmit data including their unique identities alongside positional information in a Cartesian coordinate, using a specific modulation method to allow the estimation of the receiver's position in the room. Since the coordinate origin (O) in the local coordinate of this room often has its latitude, longitude, and altitude in the global coordinate, the position of the receiver can be transferred to a global coordinate.

Figure 2 shows a general architecture for the LED-based IPS where the infrastructure has an optical driver as well as a processor while a decoding unit and a positioning estimator unit are fundamental at the receiver. The final position is presented to the user via user interface (UI) in Figure 2.

The localization process usually consists of three phases:

Phase 1: The processor obtains a communication packet from an access point (AP) controlling platform and encodes the packet data to a binary sequence. Such represents high-low voltage so that the intensity of the light can be controlled through on-off switching, also known as "on-off keying" (OOK). This modulation method is common in VLC and is usually called "intensity modulation" (IM). Normally, the packet has over 30 bits, which consists of the following parts: i) a preamble to inform the receiver of the head of the packet, ii) identification (ID) and coordinates of the transmitter, iii) an error correcting code or "cyclic redundancy code" (CRC) [33], and iv) the end of the packet. Many indoor localization systems involve two or more LEDs in a room which means the receiver can observe several transmitters at the same time. In this case, multiplexing protocols are required to combine multiple signals into one signal over a shared medium.

Multiplexing protocols, such as "frequency division multiplexing" (FDM) and "time division multiplexing" (TDM) have been widely discussed in literature. The details of these and other relevant protocols will be given in Section III. Since most LED positioning systems utilize indoor illumination as anchors, the visible light sources are mostly white LED lights. There are two mainstream producers of white lights currently on the market: i) a white LED mixed with red, green, and blue LEDs, and ii) a yellow coated LED with blue signal only, creating an overall white emission that produces broad spectrum light. The work [34] demonstrated that adopting the latter LED approach as the "triplet" was more complex and challenging in maintaining color balance. Since a phosphor component produces a much lower bandwidth (2 MHz), a blue filter may be adopted to block the phosphor component. However, this approach could impair illumination quality, as such transmitter or receiver equalization can be introduced to solve this issue [35]–[37].

Phase 2: During the positioning, in order to transmit signals via the VLC channel, the channel should consist of any line-of-sight (LOS) paths from the lights to the receiver since the LOS components are fundamental for positioning algorithms in IPS. Otherwise, the system may be severely influenced by inadequate signals. For example, the research [60] placed some obstacles in the testbed to block the LOS links. While a positioning error of 14.8 cm was reported when there was no obstacle, the block of LOS resulted in 22 cm accuracy. The system is also vulnerable to reflection components, especially in corner areas in the environment surrounded by walls and glasses. This effect will be discussed in Section III.

Phase 3: The final phase in the localization process is to estimate the location of the receiver. When the signal arrives at the receiver, some of its characteristics (e.g., RSS, TOA, and AOA) are measured and sent to the localization module as the inputs. Similar to other indoor positioning technologies, positioning algorithms (e.g., proximity and triangulation) are employed to convert them into locations. For LED-based positioning algorithms, the channel model describes the relationship between the light signal strength and distance together with other necessary parameters, such as LED power, Lambertian order, the photodiode area of the receiver, the irradiance angle, and the incidence angle [32]. This fundamental model will be discussed in detail in Section III.

During the estimation, noises are also modelled in order to reduce their influences on the positioning accuracy. Furthermore, optimization steps can be adopted using constrained conditions, i.e., movement, the range of the receiver, or the effective radius of the illumination source [38]. These positioning algorithms are often integrated into the navigation software on smart devices. In practice, LED-based positioning solutions can be integrated with other positioning solutions via a hybrid positioning scheme. Finally, the positioning results are presented to the users in indoor maps.

III. Characteristics of LED Indoor Positioning System

Because a visible light positioning system is an optical wireless system, it has many different characteristics when compared to other positioning systems using radio signals. Therefore, an accurate and robust indoor positioning system should be properly designed. In the following section, the most fundamental features will be shown and discussed in detail supported by research examples.

A. Channel Model

In visible light positioning systems, signals are transmitted from LED lights to the receiver through a free-space channel. The LED, with a large beam divergence, is often considered as a Lambertian source [39]. Thus, it broadcasts signals following Lambert's emission law, i.e., the radiant intensity or luminous intensity, observed from an ideal diffusely reflecting surface or ideal diffuse radiator, is directly proportional to the cosine of the angle between the direction of the incident light and the surface normal [33], [40]. Since the channel involves both LED and the receiver, it could be described as follows [32]:

$$P_i(\theta, \psi) = \frac{(m_i + 1)A_R P_{T_i}}{2\pi} \cdot \frac{\cos^{m_i}(\theta) \cos^{M}(\psi) T_s(\psi) g(\psi)}{D_i^2} \tag{1}$$

where D_i is the distance between the i^{th} LED and the receiver, A_R is the effective area of the PD at the receiver, P_{T_i} is the optical power of the luminance source, θ is the angle of irradiance, ψ is the angle of incidence at the receiver, $T_s(\psi)$ is the gain of an optical filter, and $g(\psi)$ is the gain of an optical concentrator placed in front of the detector [41]. M and m represent Lambertian orders of the detector and LED chip, respectively. They can be given by:

$$m = -\ln 2 / \ln\left(\cos \theta_{1/2}\right) \tag{2}$$

$$M = -\ln 2 / \ln\left(\cos \psi_{1/2}\right) \tag{3}$$

where $\theta_{1/2}$ and $\psi_{1/2}$ are semi-angles at half power of the LED and receiver. If no lens are used at the receiver, then $T_s(\psi) = g(\psi) = 1$. The optical element has a maximum "gain", which is limited by constant radiance considerations [34]. The increase of A_R will enlarge the photosensitive area to receive more lights, and therefore increases the sensitivity. However, A_R should not be too large since increasing the capacitance will decrease the bandwidth. Therefore, A_R is a tradeoff between sensitivity and bandwidth. The impact of various sizes of PD on positioning systems was shown in [42]. In this research, the influence of PD area on the accuracy of distance (PD to LED) estimation was evaluated using Ziv-Zakai bound (ZZB). For 1 W optical power, ZZB was 0.5 m when PD area was 0.01 cm^2, while the bound was 0.2 m for a PD area of 1 cm^2.

As for Lambertian orders, many researches simply set $M = 1$, based on the assumption that the half power semi-angle of the receiver is 60° [17], [33], [43]. Meanwhile, the half power angle of the LED is usually provided on the product brochure, thus the Lambertian order m can be calculated.

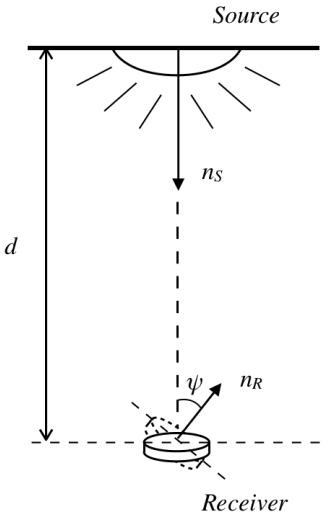

Fig. 3. A method to obtain Lambertian orders of the LED and receiver by measuring the light intensity while rotating the receiver.

However, the order M is different for various receivers, and m can slightly deviate from the calculated result, which means that estimation and reconfirmation processes will be necessary. Based on Eq. (1), in order to obtain M, it is required to measure the light intensity at multiple incident angles in a certain distance while keeping the irradiation angle strictly at 0° to fix the value of $\cos^m(\theta)$, as illustrated in Figure 3. Then, the result is compared with the Lambertian radiation pattern. Similarly, m is estimated by measuring the light intensity at different irradiation angles with the incidence angle $\psi = 0$. The work [32] has experimentally determined the parameters in the channel model for various angles, as shown in Figure 4. It can be observed from this figure that the curves generated from the measured data match well with Lambertian pattern when $M = 2$ and $m = 2.99$.

The relationship between m and the positioning accuracy was studied in [44] using Cramer-Rao Bound (CRB). In the case of 0° irradiance angle, 0.9 W optical power, and 3 m distance, the CRB of the estimated distance error between the receiver and LED dropped from 0.05 m to 0.01 m as m increased from 30 to 80. It is because the signal is more concentrated when m is larger, indicating a higher SNR [44], which is shown in Eq. (2). In [42], an opposite relationship between those two factors was reported since the irradiance angle in the simulation was non-zero but quite large (from 45° to 60°). In this scenario, based on Eq. (1), a larger m means faster power decay for a large irradiance angle, which causes a lower SNR. The distance accuracy will finally affect the 2D and 3D positioning accuracy in the positioning algorithms, such as trilateration and multilateration.

The light source is usually packaged in a lens. The radiation pattern is affected by the lens shape, the internal refractive index of the lens, and the LED arrangement [40]. Hence, an optical gain for the transmitter is considered in the model. The researches [40], [45], and [46] replaced the Lambertian order, optical filter, and concentrator gain in Eq. (1) with exponential orders on the account of using a lens for both LED and

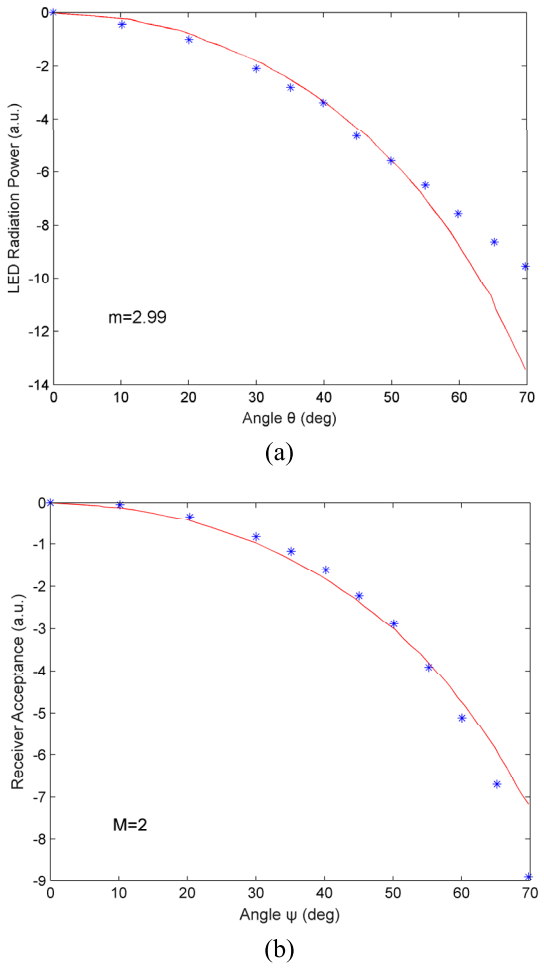

Fig. 4. Experimental measurements (blue asterisks) to show the relationship between received light power and angles. (a) Lambertian radiation pattern of the reference LEDs and (b) angular acceptance of the receiver. Both curves are fitted with the Lambertian function (red solid line) [32].

PD. Thus, Eq. (1) is converted to the following equation:

$$P_r = \left(P_t/d^2\right) C_{opt} G_t(\theta) G_r(\psi) \tag{4}$$

where $G_t(\theta) = \exp(-\theta_{S_t}/k_t)$ and $G_r(\psi) = \exp(-\psi_{S_r}/k_r)$. S_t and S_r are slope constants which are determined by lens shapes of transmitters and the receiver, respectively. k_t and k_r are related to $\theta_{1/2}$ and $\psi_{1/2}$ by $k_t = (\theta_{1/2})_{S_t}/\ln(1/2)$ and $k_r = (\psi_{1/2})_{S_r}/\ln(1/2)$, respectively.

The channel model provides a reliable description of the propagation of optical signals. In real situations, however, the optical signals often reach the receiver by both direct LOS and multiple reflected paths. This means that there is no simple way to determine the distance or direction of the transmitter from the received signals. Hence, the essential features of the IPS will be discussed in the rest of this section to model a more robust optical channel.

B. Multiplexing Protocols

VLC has shown that LEDs can be used for lighting and communication characteristics simultaneously. Due to its advantages, such as avoiding radiation and electromagnetic

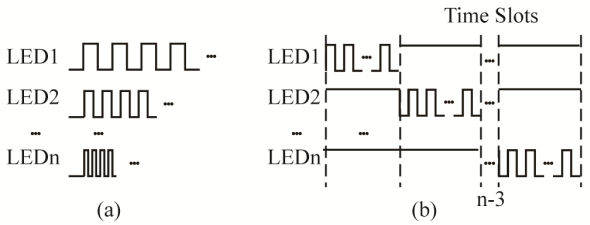

Fig. 5. Frame sequences of multiplexing protocols. (a) FDM-IPS frame sequence, (b) TDM-IPS frame sequence.

interferences (the wavelength of microwave is thousands times larger than the 650nm wavelength of visible light), LEDs have become a high speed wireless source in IPS technology. The performance of current LED-based IPSs, however, is limited by the demodulation bandwidth of VLC, especially for multi-source scenarios. Here, the multi-path transmission is extremely challenging for IPS receivers with limited processing capability, such as "complementary metal oxide semiconductor" (CMOS) cameras. Several multiplexing methods (i.e., TDM, FDM, polarization multiplexing, and space divided multiplexing) have been developed for VLC technology to transmit in parallel, and thereby effectively enhance the transmission capacity of the system. In LED-based IPSs, LED beacons usually have to modulate and transmit data, which contains necessary parameters like ID, coordinate information, and transmitted power, in order to help the receiver calculate its distance to the LEDs. However, multiple LEDs in the system transmit their data packages at a high modulating speed. Hence multiplexing protocols with respect to VLC technology are required by visible light based IPSs to ensure the receiver can correctly extract the information.

FDM and TDM are widely adopted in LED positioning systems [16]–[18], [38], [47]–[49]. The FDM protocol divides the total bandwidth available in the VLC medium into a series of non-overlapping frequency sub-bands corresponding to the number of used LEDs, each of which is used to carry a separate signal, as presented in Figure 5 (a). Figure 5 (b) shows the TDM protocol, which separates the overall time into several time slots. In this case, each LED signal appears only in one slot and synchronously switches at each end of the transmission line.

As far as multiplexing protocols are concerned, much work is required to overcome the limitations of FDM and TDM. For example, to enhance the independence of multi-access signals for FDM protocols, Orthogonal Frequency-Division Multiplexing (OFDM), which is mainly adopted in RF based wireless communication systems such as current fourth generation (4G) communication, has been employed in LED localization [32]. OFDM uses several closely spaced orthogonal signals to cope with severe channel conditions such as narrowband interference and multi-path frequency-selective fading.

On the other hand, many LED-based localization methods using TDM protocols or TOA algorithms are influenced by imperfect synchronization among the LEDs and receivers. IEEE 802.15.7 uses the synchronization header in

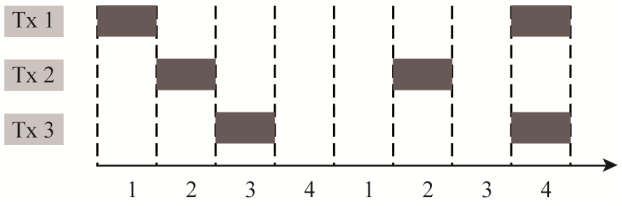

Fig. 6. Basic frame slotted ALOHA protocol (three transmitters, four slots per frame). Noted that in the second frame, signals of Tx1 and Tx3 are overlapped in the fourth slot.

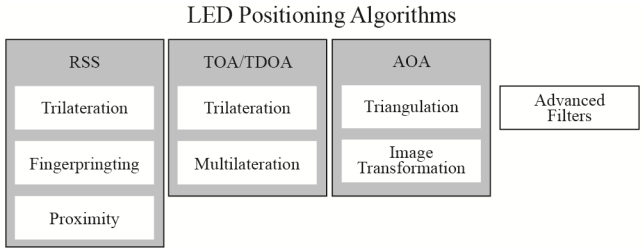

Fig. 7. Taxonomy of LED positioning algorithms.

the data frame to help the receiver and LEDs adjust their clocks during positioning. However, the clocks of transmitters are difficult to be synchronized since LEDs cannot receive signals from each other [21]. A modified Additive Link Online Hawaii System (ALOHA) protocol, called Basic Framed Slotted ALOHA (BFSA), has therefore been adopted to eliminate the need for total synchronization. This defines a frame structure composed of a fixed number of time slots, which are usually much larger than the number of transmitters as shown in Figure 6. Each transmitter randomly selects a slot in the length of a frame to transmit data [50].

When appropriate modulation in multiplexing protocols to IPS is applied, it is worthy to note the following aspects:

i) Avoiding visible flicker is of primary importance as the basic function of the LEDs is energy-efficient illumination; therefore, the frequency of the on-off keying must be above 200 Hz, and can be 10MHz, in order to prevent discomfort for human eyes.

ii) Multiplexing protocols should not compromise the luminance quality, thus an appropriate modulation method should be adopted. Traditional modulation like Pulse Position Modulation (PPM) often adopts high voltage to present "1" in data transmission. Since the light intensity corresponds to the duty cycle of the luminance source, PPM modulation could yield relatively low brightness if the data sequence is too sparse. A variant of this modulation method called Inverted-LPPM (I-LPPM) can be used to cope with this situation, mainly by inverting the pulse position of the PPM modulation [51]. Consequently, the average transmitted power of the LED is enhanced, yielding a relatively high luminance quality. In fact, IEEE 802.15.7 specifies variable pulse position modulation (VPPM) to prevent flickering problem and provide a dimming control mechanism for VLC. To date, VPPM has been applied in few positioning systems, and therefore requires further researches.

C. Field of View

Technically, the receiver only senses the light lobes within its Field of View (FOV); therefore, a receiver with a wider FOV is used for a large-scale indoor environment. A wider FOV, however, results in receiving more undesired signals from non-line-of-sight (NLOS) reflections or ambient light, which may lead to performance degradation [41]. Hence, a trade-off needs to be made for the choice of FOV in the IPS design. In this section, the impact of FOV and its choice for IPS design in relevant research will be discussed and there is a significant distinction between the PD and image sensor.

Because VLC LOS luminance lobes are much greater than diffused and reflected components, its LOS part is less affected by noise when compared to radio signals. Nevertheless, the presence of large noise can still hamper the localization accuracy of VLC-based IPSs. The research [52] showed that the 2D RMS positioning errors were 46.3 cm, 33.6 cm, and 29.8 cm for receiver FOV angles of 25°, 17.5°, and 10°, when using a single PD as the receiver. This research showed that accuracy was degraded by an increase in the FOV. In another research [38], the system was tested using PDs of different FOV between 70° and 100°, and the simulation result showed that the FOV angle of 90° provided the most accurate "mean Euclidean distance". It was perhaps because the receiver with a smaller FOV could not receive enough light sources to provide a positioning solution, while the receiver with a larger FOV could gain a greater amount of ambient light and reflections. Given these results, it is a trade-off to select the parameter FOV of PD for IPS applications.

This pattern for PDs, however, cannot be applied to image sensors. Although the image sensor is fabricated by an array of PDs, the positioning methods using the image sensor in the IPS design are different from those using PDs. The PD converts the flux from light to electric current; therefore, a single PD only provides the information of RSS or TOA. On the contrary, the image sensor is capable of providing AOA by using certain image processing technology. The image sensor consists of CMOS arrays with a microlens, approximately positioned with a distance of focal length to its front, so that when the flux from the light source passes through the lens, i) the concentrated location of the flux on the CMOS arrays, ii) the microlens center, and iii) the light source are co-linear. Then, the irradiance angle θ can be calculated if i) the location of the light source on the photos, ii) the size of the CMOS arrays, and iii) the focal length of the microlens are known. It is necessary for the receiver in the camera-based IPS to cover all required luminance sources within its FOV. Since the AOA-based positioning algorithm is not disturbed by luminance flux from reflection and other lighting sources, it is preferred to set the FOV of the camera as large as possible, which is different from the PD. The research [53] reported an improved positioning accuracy for the image receiver with an ultrawide-FOV microlens, which improved the accuracy from 3.2 cm to 1.5 cm when compared to the receiver with the wide-FOV microlens. This relatively small positioning error is achieved by using ultrawide-FOV receivers based on the fact that the lobes can be more perpendicular at their intersection for ultrawide-FOV receivers in the case of

closely-spaced optical sources. On the other hand, for small FOV microlens, the incident lobes become nearly parallel at their intersection, yielding a large positioning error. To satisfy customer's photography demands, smartphone manufacturers make the field of view for the attached cameras wider to achieve a higher performance in their productions, thereby creating great benefits to camera-based IPSs.

D. Noise

Because Signal-to-Noise Ratio (SNR) is essential to evaluate the performance of the VLC systems, the noise in an LED-based positioning system should not be neglected. Many LED IPSs report large positioning errors (above 0.4 m) in the outer region, i.e., outside the area surrounded by the LEDs, or marginal area [54]. This is mainly because the light power received from far-off LED transmitters is largely degraded by the long distance travel and a large irradiance angle, which is quite comparable to the noise and leads to a relatively low SNR in the area. The PD current is mainly affected by two kinds of noise. The first one is shot noise which is the fluctuation in the electric current due to incident optical power including the desired signal and other light sources in the environment, given by:

$$\sigma_{shot}^2 = 2q\gamma(P_{rec})B + 2qI_{bg}I_2B \tag{5}$$

where q represents electronic charge, γ is the detector responsivity, B is equivalent noise bandwidth, I_{bg} is current caused by background disturbance, I_2 is the noise bandwidth factor [41]. P_{rec} is given by

$$P_{rec} = \sum_{i=1}^{n} H_i(0)P_i \tag{6}$$

where $H_i(0)$ is the channel DC gain, n represents the number of LEDs, and P_i is the instantaneous emitted power for the i^{th} LED bulb. Ambient light such as artificial lights or sun lights can have a direct impact on the shot noise, resulting in larger background current. The typical current is 5100 μ A under direct sunlight exposure and 740 μ A under indirect sunlight exposure [55].

The second noise is the thermal noise which is the current fluctuation caused by the rising temperature of the electric circuit when the receiver works. The thermal noise variance is given by

$$\sigma_{thermal}^2 = \frac{8\pi kT_k}{G_o}\eta AI_2B^2 + \frac{16\pi^2kT_K\Gamma}{g_m}\eta^2A^2I_3B^3 \tag{7}$$

where the first part represents feedback-resistor noise and the second part is field effect transistor (FET) channel noise. k is Boltzmann's constant, T_K is the absolute temperature, G_o is the open-loop voltage gain, η is the fixed capacitance of photodetector per unit area, A is the effective area of PD, Γ is the FET channel noise factor, g_m is the FET transconductance, and I_3 is the noise bandwidth factor. Based on Eq. (6) and Eq. (7), it can be seen that the equivalent noise bandwidth B can directly influence the quantity of both noises, and further affect the positioning accuracy. Theoretical analysis of this influence was studied in [44]. When the optical power was 1W and $B = 800MHz$, CRB achieved 6 cm in the distance of 3 m with $\sigma_{thermal}^2 = 1.1\times10^{-13}A^2$ and $\sigma_{shot}^2 = 1.9\times10^{-18}A^2$. In the case of $B = 100MHz$, the CRB dropped to less than 1 cm.

The total noise variance, σ_{noise}^2, in electric current domain is given by

$$\sigma_{noise}^2 = \sigma_{thermal}^2 + \sigma_{shot}^2 \tag{8}$$

Generally, the effective SNR in the electric current domain generated from the LOS component is defined as

$$SNR(dB) = 10\log_{10}\frac{\left(R_p\frac{P_{LoS}}{A}\right)^2}{\sigma_{noise}^2} \tag{9}$$

where R_p and A are the responsivity and effective area of the PD, respectively. Under direct sunlight exposure, a minimum value of 39.5 dB SNR was reported in [56] in a 5×5 m^2 room with 16 LEDs (0.452 W, 355.6 lx). SNR can reach 59 dB when the illuminance is 1712.8 lx. 300∼1500 lx is required for working environment by ISO standards. The work [54] reported a maximum SNR of 50 dB at the room center and a minimum SNR of 34 dB on the corner under indirect sunlight. In this case, the average positioning error was 5.9 cm. Under direct sunlight, an overall reduction of 5 dB occurred on the SNR, achieving 14.3 cm mean positioning error.

Usually, the dominant component of the noise at the receiver is the shot noise, since most systems operate in the presence of high ambient light levels [57]. Thermal noise is often negligible compared to shot noise for large-area optical receivers [17]. Furthermore, some methods are proposed to reduce the influence of the noise in the positioning system, such as increasing the power of the luminance source [58] and using a filter to reduce the noise component [43].

E. Multipath Effect

Since LED is an illumination source, luminous fluxes are dispersed around the room. This creates reflecting components from the walls, ceilings, tables, mirrors, and any other surfaces within the room. Although the reflecting components are much weaker than the LOS channel, due to multipath effect, they are still perceptive to the optical sensor and may contribute to a diffuse channel in the VLC system which will influence SNR, "Bit Error Rate" (BER), and other system performance metrics. The article [59] studied time dispersion for different surfaces with different reflectivities. LED-based positioning systems can also be affected by multipath effect. The effects on RSS-based and TOA-based positioning systems were studied in [60]–[63].

RSS-based IPSs perform positioning by transferring received light power to distances. Therefore, the distance estimation will become worse if the reflected components are mixed into the received signals, leading to a larger positioning error. In the research [62], simulation results showed that impulse response of the first reflection was around one-fifth of the LOS part, when the receiver was 0.2 m from the walls. This led to a positioning accuracy degradation from 14.06 cm to 1.52 m. Results also showed that the localization accuracy was gradually improved as the increase of the transmitted power

if there were no NLOS signals. However, under multipath effect, increasing transmitted power would not significantly improve the accuracy as the localization error quickly achieved a stable value. In the work [60], the impulse response of the optical channel was calculated with a combined deterministic and modified Monte Carlo method. This study simulated the received signals at different locations inside the room. On the corners or edges, comparing with the LOS part, strong reflecting parts were only delayed by few nanoseconds. The amplitudes of the first reflections were almost comparable to the LOS part. The impact of such a multipath on the positioning error was also quantified in the simulation. On the corner, the positioning error was 1.7 m when reflection factor of the wall was 0.66, while the positioning error was only 9.8 mm if no reflection.

The impact of the multipath effect on a TOA system was studied in a NLOS environment [63]. This system generated prior information of the NLOS distribution using NLOS propagation-induced path lengths modeled by gamma distribution [64]. Generalized Cramer-Rao lower bound (G-CRLB) was derived as the positioning accuracy and results showed that when NLOS delays were neglected, the accuracy was degraded from 1 cm to 3 cm with 10 W transmission power.

F. Error

Errors in the basic parameters in LED-based designs, for instance, asynchronization in time multiplexing protocols, inaccurate angle measurement caused by poor image processing or inertial sensors, and imperfect installation of the LED infrastructures, can cause a huge impact on system performance.

The TDM-based designs are very sensitive to timing synchronization errors when all transmitters are operating. Since the signals from different LEDs are transmitted with the same power, but in different time slots, the received signal in each slot, ideally, does not consist of other components. However, if there is a timing synchronization error between two LEDs transmitting signals in neighbouring slots, this error can be modelled as:

$$\hat{P}_1 = P_1 + \alpha P_2 + \frac{2}{P_T} n(t) \tag{10}$$

$$\hat{P}_2 = (1-\alpha) P_2 + \frac{2}{P_T} n(t) \tag{11}$$

where P_1 and P_2 represent the received light intensity of two LEDs, α is the synchronization error percentage, $n(t)$ is the noise at the receiver, $\hat{P}_1$ and $\hat{P}_2$ are the actually received power intensity in each slot. Eq. (10) and Eq. (11) show that the received power in each slot is higher or lower than the actual value, which would reduce the accuracy of the estimated distances from RSS values. Therefore, RSS-based positioning algorithms should make allowances for this error if TDM protocols are used. The research [47] analyzed the impact of timing synchronization errors by assuming that only two of the LEDs are out of synchronization by a certain percentage. The positioning performance with a synchronization error of 5% and 10% was 13.7 cm and 24.6 cm, while the localization error was 9.1 cm for fully synchronized TDM IPS. This result showed a significant degradation of positioning accuracy as the synchronization error increases.

Many camera-based positioning systems rely on image processing quality, which is heavily limited by the features of the camera. Firstly, the estimated LED's location on the image could slightly deviate from the actual coordinates due to the limited resolution of the image. However, a relatively small error of the LED's location on the image can result in a large observation error in the LED's location in the real world. Therefore, the calculated LED location becomes more accurate when the size of the pixel reduces [31]. Secondly, for a large and unstable environment, the photographing might be extremely obscure due to poor exposure and filter, which means that the location of the light source on the image is difficult to determine. Finally, the AOA of the signal can be fairly inaccurate, thus yielding a large localization error in the positioning algorithm. Quantization error in image processing, which is caused by setting a threshold for determining the light intensity in pixels, further hampers the system.

IV. LED Positioning Algorithms

RF-based positioning algorithms have been developed for indoor positioning systems and these are also applicable to LED-based positioning systems. In this section, these approaches are classified into the following four categories (which is shown in Figure 7): i) RSS, ii) TOA/TDOA, or iii) AOA and iv) advanced filters. In each category, we have looked further into the applicable algorithms, some of which might have overlapped with other categories. However, how these algorithms leverage these characteristics is different, and details are given as follows.

A. Received Signal Strength

RSS-based methods have been widely employed in indoor positioning systems and visible light systems. Compared to other characteristics of transmitted signals, RSS values are easy to obtain using a single photo-detector without the need for auxiliary devices. Normally, the received signal intensity follows the channel model, which means that the intensity is reduced as the distance between transmitter and receiver increases. Based on this model, many algorithms can be applied for LED positioning systems, such as trilateration, fingerprinting and proximity, with many published articles verifying these approaches.

1) Trilateration: Positioning algorithms based on trilateration should use at least three LEDs with known locations in the system [18], [33], [40], [43], [48]. In this section, a typical case for using three LEDs is introduced for demonstration purpose. Once the receiver has measured the intensity of the transmitted signals, each distance from the corresponding transmitter is calculated and circles with the radii of calculated distances can be drawn. The location of the receiver can then be determined by calculating the intersection point of the circles, as depicted in Figure 8. This process usually appears

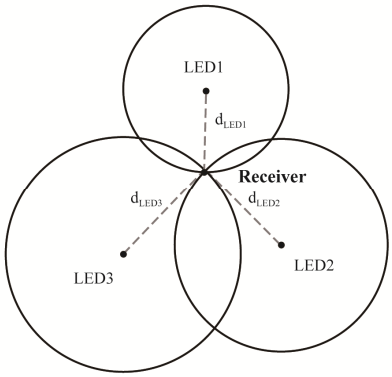

Fig. 8. Trilateration (intersect in one point).

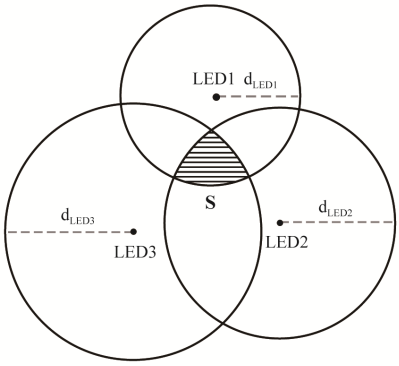

Fig. 9. Trilateration (intersect within an area).

as a simultaneous equations problem, as follows:

$$\begin{cases} (x-x_1)^2+(y-y_1)^2=d_1^2 \\ (x-x_2)^2+(y-y_2)^2=d_2^2 \\ (x-x_3)^2+(y-y_3)^2=d_3^2 \end{cases} \tag{12}$$

Due to existing quantization and measurement errors, the measured distance usually deviates slightly from the ground truth. Therefore, for most cases, the drawn circles do not intersect perfectly and the intersection points margin an overlapped area, like the shadow in Figure 9. This is actually a least square estimation problem [54]. The discussion above is a 2D localization, which is under the assumption that all the LEDs are installed at the same height ($z_{LED_1} = z_{LED_2} = z_{LED_3}$) and that the z coordinate of the receiver is also known. It is noted that large installation errors (5%) can severely affect the positioning accuracy, as a 20 cm higher error reported in [49] and [54]. In 3D localization, three unknown coordinates should be determined. In this case, the intersection point is formed by three or more spheres. Furthermore, the hatched area in Figure 9 becomes a space with certain volume. To deal with this problem, the receiver should contact at least four transmitters, leading to four quadratic equations.

2) Fingerprinting: Fingerprinting-based indoor positioning systems usually consist of two steps: i) off-line survey, and ii) on-line positioning [4], [47], [65]–[68]. At the off-line survey stage, specific information of the indoor environment, such as AOA, RSS, or TOA of the signal, is collected, processed and recorded in the database. At the on-line positioning stage, the target is located by comparing the received information with that in the database.

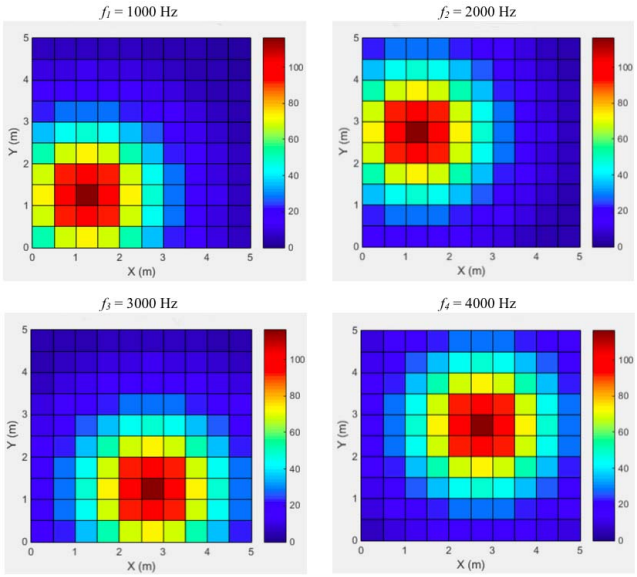

Fig. 10. Simulated fingerprint database of four LEDs, which are located at (1, 1, 3), (1, 2.5, 3), (2.5, 1, 3), and (2.5, 2.5, 3) in the room.

Current LED IPS designs mainly adopt the RSS-based fingerprinting algorithm [47], [66]. The indoor map is divided into a self-defined grid containing several points called fingerprint locations. During the off-line stage, the RSS values from observed LEDs are collected at each location. This process is labor-intensive; therefore, it is important to choose an appropriate grid size for the fingerprint database (see Figure 10). Welch's method can be used to determine the Power Spectral Density (PSD) of the received signal [66]. The power at each LED frequency is extracted by a band pass filter (BPF), where the extracted power is recorded as a reference for each LED and uploaded to the database in the positioning server. During the on-line stage, the photo detector records RSS from LEDs at the location of the target. The Euler distance is usually used to calculate the difference between the measured RSS values and those in the fingerprint databases, which is given as follows:

$$D(\mu, i) = \sum_{j=1}^{V} \left(\mu_{o,j} - \mu_{i,j}\right)^2 \tag{13}$$

where $i = 1, 2, \ldots, N$ refers to the fingerprints in the database, $j = 1, 2, \ldots, V$ refers to the modulating frequency for different LEDs, $\mu_{i,j}$ is the RSS value of i^{th} fingerprint for j^{th} modulating frequency in the database, $\mu_{o,j}$ is the observed RSS value at the observation location for j^{th} modulating frequency. Finally, the location of the target is determined by the location of the fingerprint that yields the smallest Euler distance. Sometimes, however, transmitters may vary in emitted power, which influences the RSS values in the fingerprint map and ultimately affects the positioning accuracy. This effect can be reduced by introducing a normalization factor [66].

a) Deterministic methods: Most systems adopt k-Nearest Neighbors (k-NN) to estimate locations with

fingerprints [66], [69], [70]. In [70], the RSS-based fingerprinting algorithm was combined with multiple classifiers, including random forest, *k*-NN and extreme learning machine (ELM), to yield a better location prediction. Simulation results showed that this system achieved less than 7.5 cm accuracy, which was only 37.5% of the regular RSS matching method (20 cm).

b) Probabilistic methods: while the k-NN algorithm is usually classified as a *deterministic* fingerprinting positioning algorithm, another branch in fingerprinting algorithms is the *probabilistic* positioning algorithm. It differs from the deterministic algorithm in that, instead of storing certain RSS values, it stores the probability distribution of the RSS and uses the Bayesian method to calculate the user's location. The research [71] proposed a probabilistic positioning system to address the issues of illumination occlusion and synchronization error. By introducing noise and shadowing factors in the stochastic model, the system obtained 0.81 m accuracy in a 30×30 m^2 simulated floor.

3) Proximity: Proximity algorithms have so far been used in infrared radiation (IR), RFID and Bluetooth, providing symbolic relative location information [72]–[74]. Usually, when a target receives signals from the transmitters with known locations, it is considered to be close to them. By comparing the RSS values of these signals, the transmitter with the strongest signal is considered to be nearest to the target, and its location is selected as the rough estimation of the target location. If there are multiple signals with the same intensity, the target is considered to be in the middle of these transmitters. Unlike other positioning approaches, this method is relatively easy to implement; however, it is not very accurate since the method relies heavily upon the density of the transmitter distribution. Normally, indoor LED lamps are positioned 2 or 3 meters from each other, therefore, this method might be applicable in situations where coarse estimations are sufficient.

B. Time of Arrival/Time Difference of Arrival

TOA, the absolute travel time of a wireless signal from the transmitter to the receiver, is an important technique in localization which is often used in GPS [75]. However, it requires very accurate time synchronization between LEDs and receivers. Therefore, to avoid the need for accurate time synchronization, indoor localization systems usually adopt time-difference-of-arrival (TDOA) instead of TOA. However, it is noticeable that time synchronization is still required among LEDs. Typically, the TDOA system needs at least two receivers to acquire the time difference between the receivers. Nevertheless, with the help of multiple LEDs modulated in FDM and using a BPF on the receiver side, a single receiver is capable of acquiring signals separately and analyzing the time difference between all the signals, leading to a practical application for TDOA-based IPS.

1) Trilateration: TOA/TDOA-based positioning also can employ trilateration algorithms based on grounds that because the light travels at the constant speed over a certain distance, it causes phase delay in the receiver. At least three phase differences are required for TDOA-based systems, which means there are at least three transmitters in the system. Each transmitter is equipped with a Frequency ID (F-ID). Assuming there are three LEDs represented by $i = 1, 2, 3$, the radiated power can be expressed as:

$$P_i(t) = P_{CONT} + P_{MOD}\cos(2\pi f_i t + \varphi_0), \tag{14}$$

where P_{CONT} is the continuous optical signal, P_{MOD} is the modulated signal, and φ_0 is the initial phase of the optical signal, and $f_i = 1, 3, 5$ kHz is the modulated frequency. The received signal can be given by:

$$E(t) = K \cdot \left| R \cdot \sum_{i=1}^{3} P_i(t) \otimes h_i(t) \right|^2, \tag{15}$$

where R is the responsivity of the PD, K is the constant proportionality, and $h_i(t)$ represents the channel impulse response. Then, the signal is processed by BPFs corresponding to each modulated frequency, and the output signals are:

$$E_{BPFi}(t) = L_i \cdot \cos\{2\pi f_i(t - d_i/c) + \varphi_0\}, \tag{16}$$

where $L_i = 2 \cdot K \cdot R \cdot H(0)_i \cdot P_{CONT} \cdot P_{MOD}$, and d_i represents the distance between LED_i and the receiver. We can unify the frequency for each signal by using a frequency down converter which consists of a mixer and a BPF. The signals after the conversion become:

$$E_{SIGi}(t) = K_i \cdot \cos\{\pi f_1 t - 2 \cdot j\pi f_1 d_i/c + \varphi_{TOT}\}, \tag{17}$$

where $j = 1, 3, 5$, and φ_{TOT} is the total phase shift. Next, it is able to detect the phase difference by using Hilbert transform. Normally, only two phase differences can be acquired from three LEDs. To obtain a third phase difference, one approach proposed by [18] creates another phase difference by switching the frequency of 1st and 2nd transmitters in a certain time slot. The signals from Eq. (17) then pass through a BPF and a phase detector based on the Hilbert transform. Finally, the phase differences are extracted as follows:

$$\begin{cases} \Delta\varphi_{12} = 2\pi f_1 \frac{d_1 - 3d_2}{c} = \tan^{-1}(I_{12}/Q_{12}) \\ \Delta\varphi_{13} = 2\pi f_1 \frac{d_1 - 5d_3}{c} = \tan^{-1}(I_{13}/Q_{13}) \\ \Delta\varphi_{21} = 2\pi f_1 \frac{d_2 - 3d_1}{c} = \tan^{-1}(I_{21}/Q_{21}) \end{cases}, \tag{18}$$

where f_1 is the reference frequency, I and Q are obtained from following equations:

$$\begin{cases} I_{12} = E_1(t) \cdot Hilb[E_2(t)] - Hilb[E_1(t)] \cdot E_2(t) \\ Q_{12} = E_1(t) \cdot E_2(t) + Hilb[E_1(t)] \cdot Hilb[E_2(t)] \end{cases}, \tag{19}$$

where $Hilb[\,\cdot\,]$ is the Hilbert transform, and E is the received signal after BPF and down conversion.

In the next step, the distances are calculated based on Eq. (18), and we have:

$$\begin{cases} d_1 = -\frac{1}{8}\frac{c}{2\pi f_1}[\tan^{-1}(I_{12}/Q_{12}) + 3\tan^{-1}(I_{21}/Q_{21})] \\ d_2 = \frac{1}{3}\left[d_1 - \tan^{-1}(I_{12}/Q_{12})\frac{c}{2\pi f_1}\right] \\ d_3 = \frac{1}{5}\left[d_1 - \tan^{-1}(I_{13}/Q_{13})\frac{c}{2\pi f_1}\right] \end{cases} \tag{20}$$

Finally, the position of the receiver can be estimated by using trilateration and these distances.

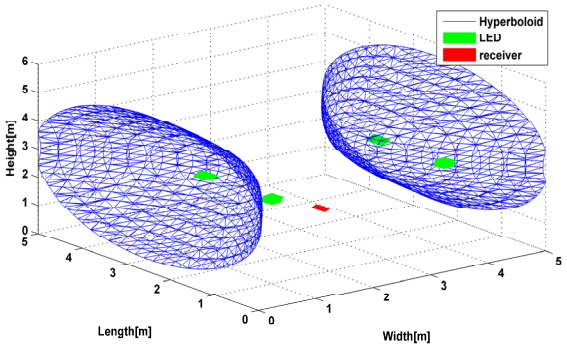

Fig. 11. Hyperboloid formed by distance differences between two LEDs and the receiver.

Under low SNR conditions, the CRB of ranging errors could be quite loose, which means in terms of actual positioning results, positioning errors of most locations are much lower than the CRB value [42]. Ziv-Zakai bound (ZZB) for synchronous IPS was derived in [42]. Unlike CRB, this extracts the ranging accuracy by utilizing the distance information and prior probability density function (PDF) along with Lambertian orders, optical power and other basic parameters. Therefore, tight limits can be obtained by ZZB for all SNR conditions including low SNRs.

2) Multilateration: Multilateration (MLAT), which is also known as hyperbolic navigation, is a navigation technique often used in TDOA-based systems [76], [77]. It is based on distance differences of any two LEDs with known locations. Multilateration is different from trilateration which uses distances or absolute measurements of time-of-flight. The distance difference between each set of two transmitters is given by:

$$d_i - d_j = \sqrt{(x_i - x_R)^2 + (y_i - y_R)^2 + (z_i - z_R)^2} - \sqrt{\left(x_j - x_R\right)^2 + \left(y_j - y_R\right)^2 + \left(z_j - z_R\right)^2} \quad (21)$$

where (x_i, y_i, z_i) represents the 3D position of the i^{th} LED, and (x_R, y_R, z_R) represents the position of the receiver. Unlike directly measured distance or angle, the distance difference between each LED transmitter and the PD is not absolute. Therefore, it could be satisfied by an infinite number of locations, which form a hyperbolic curve when plotted in Cartesian coordinates (see Figure 11). To narrow down all the possible locations, a second pair of transmitters are measured to generate another curve. Both curves may intersect in several places that are possible locations of the target and if more curves are added, the location of the target can be determined. However, due to ambient light noises and reflections, these curves usually meet in more than one point, which could be a region that contains the receiver. The problem can be solved by calculating the mean of the intersections, or using other optimization algorithms.

Related works using multilateration reported large positioning errors under shot noise and thermal noise, along with noise caused by the reflected lights from the walls [76], [77]. Different optimization algorithms can be utilized for location estimation. For instance, the Levenberg-Marquardt (LM) algorithm [76] achieved a low accuracy for the location estimation. The system was further refined by using an extended Kalman filter (EKF) and the 3D accuracy reached approximately 0.1m.

C. Angle of Arrival

AOA refers to the propagation direction of a signal incident on a receiver in the IPS design. More specifically, it is the angle between the line of sight and the normal angle of the transmitter's plane. However, AOA cannot be measured directly by a photodiode or a camera. Two approaches may be taken to obtain AOA values: i) image transformation and ii) modeling. Image transformation first takes photos of the light with a camera, and then makes use of the trigonometric relationship between the coordinates of the light beacons and the location of its image on the photo to calculate AOA [78]. This is simple if the camera is horizontally placed. Otherwise, MEMS sensors (e.g., accelerometers and magnetometers) will be used to measure the attitude (i.e., azimuth, roll, and pitch) of the camera [79], [80]. Using this approach, the camera FOV should be large enough. The image resolution and quantization error will influence the positioning accuracy. The second approach, modeling, makes full use of the channel model since the received power is related to the radiation angle [38], [58]. This approach should be employed by the photodetector rather than the image sensor. By measuring the light intensity at a certain receiver gesture, which is determined by MEMS sensors, the radiation angle can be obtained using the model equation with other preliminarily assumed parameters.

Triangulation is the most popular algorithm to determine the location using AOA [46], [49], [58], [81]. It is different from trilateration. However, many articles often refer to them as the same concept since they both use the geometric properties of triangles for location estimation. In fact, there are two branches of triangulation: i) lateration and ii) angulation [54]. The former is called trilateration, which estimates the target location by measuring its distances from multiple reference transmitters. The latter, angulation, measures angles (AOA) relative to several reference transmitters. In this article, we shall call the angulation method "triangulation" and the lateration method "trilateration". Once the AOA is obtained from the signals, the location is estimated by finding the intersection of the direction lines (see Figure 12).

Compared with TDOA and RSS, AOA-based IPS systems have many advantages, such as i) avoiding time synchronization and ii) no need to consider path loss and disturbance from background lighting sources and reflected components for image transformation approaches. AOA is always more stable if it is obtained with the aid of MEMS sensors. Furthermore, it is not widely used in radio-based systems, such as WiFi and Bluetooth, which typically have no line of sight. Therefore, AOA can be thought of as an advantage for LED-based IPSs.

D. Advanced Filters for Data Smoothing

All of the aforementioned localization algorithms require LOS between the transmitter and the receiver. In real situations, however, there might be an insufficient number of

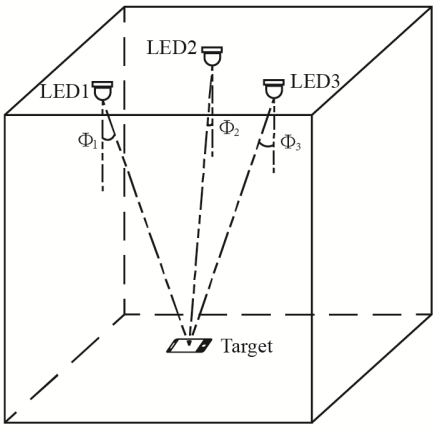

Fig. 12. Triangulation method.

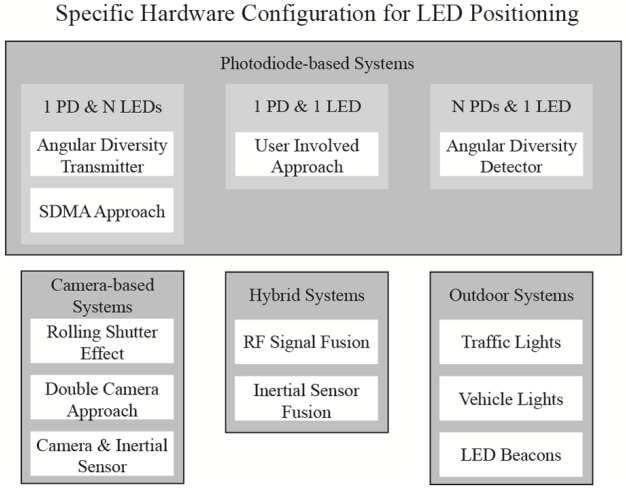

Fig. 13. Classification of specific LED positioning applications.

light sources, especially in complex and crowded indoor environments, resulting in positioning failure. Additionally, direct LED positioning usually shows unsmoothed results even when people are walking straightly and smoothly. In these situations, filtering technologies are often employed to improve the performance of the real-time tracking of the target. In relevant research, two sorts of filters are adopted – the Kalman filter (KF) and the particle filter (PF) [43], [81], [82].

The KF is widely used in positioning systems and is based on the assumption that the systems are Gaussian and linear [83], [84]. In LED positioning systems, shot noise and thermal noise are the main sources of noise and both are assumed to be Gaussian white noise, approximately meeting the KF requirements. The KF algorithm, which is shown in Table II, includes two phases. The first one is the prediction phase, which involves using the last state and covariance to predict current state and covariance. The second phase is the update phase, which modifies the prediction result by adopting new measurements. These phases are recursively operated to improve positioning accuracy. The research [43] adopted the KF to smooth the route in navigation, where the position measurements were from trilateration. In the proposed algorithm,

TABLE II
KALMAN FILTER ALGORITHM

Input:

$\{s_{k-1}, P_{k-1}\}$ **: state and covariance at time step** $k-1$

m_k **: measurement at time step** k

Output:

$\{s_k, P_k\}$ **: state and covariance at time step** k

Process:

1) Prediction

generate the next state and covariance

$$s_k^- = A s_{k-1} + B u_k$$

$$P_k^- = A P_{k-1} A^T + Q$$

2) Update

compute Kalman gain, update state and covariance

$$K_k = P_k^- H^T \left(H P_k^- H^T + R\right)^{-1}$$

$$s_k = s_k^- + K_k \left(m_k - H s_k^-\right)$$

$$P_k = \left(I - K_k H\right) P_k^-$$

the state s_k was composed by the horizontal position and velocity, which were initiated by using the initial position from the trilateration method and assuming zero velocity at the beginning of the navigation. Then the state is predicted based on the former state and kinetic model. A is the matrix determined by the kinetic model. u_k represents the process noise vector, which is assumed to be Gaussian and zero mean. The covariance P is predicted simultaneously in both prediction phase and update phase. The Kalman gain is calculated from the predicted values. Then, the state and covariance are updated by using the measurements from VLC positioning. The updated state will then be outputted as current position and velocity. The prediction and update phases are then iterated in order to keep generating position information. The simulation result in [43] showed that the RMS positioning error decreased from 0.143 m to 0.115 m by exploiting KF when the raw measurement had a jump point which was approximately 2 m away from the movement trace.

The KF achieves an optimal estimation performance for a linear system. For a non-linear system, however, advanced KF, such as extended Kalman filter [85]–[87] and unscented Kalman filter [88], [89] should be used to achieve an improved estimation solution.

In fact, the system model in KF can use the kinetic model to lower the effect of system noise and further avoid large deviation of the estimated route. The measurement model utilizes VLC measurements to adjust the movement parameters. Therefore, KF is introduced in many other positioning methods besides trilateration. The research [81] applied KF to optimize the triangulation positioning based on AOA. The research [76] introduced EKF in the TDOA-based multilateration positioning.

The PF (see Table III), which is a Monte Carlo method, uses a set of weighted particles to approximate the real posterior

TABLE III
PARTICLE FILTER ALGORITHM

Input:

$\left\{x_{k-1}^i, w_{k-1}^i\right\}$ **: particles at time step** $k-1$

z_k **: measurement at time step** k

Output:

$\left\{x_k^i, w_k^i\right\}$ **: particles at time step** k

Process:

1) for each particle x_{k-1}^i

generate the new particle x_k^i **using the channel model**

$p\left(x_k^i \mid x_{k-1}^i\right)$

2) for each new particle x_k^i

compute the new weight using the measurement model

$w_k^i = w_{k-1}^i p\left(z_k \mid x_k^i\right)$

3) Normalizing the new weight $w_k^i = \dfrac{w_k^i}{\sum_{j=1}^{N_S} w_k^j}$

4) resampling

distribution [90]–[93]. During the process, both particles and their weights are predicted. A resampling process is usually used in PF to prevent the degeneracy problem [85]. Unlike KF, linearity and Gaussian distribution are not required in PF process [90]–[93]. In [43], particles are generated from a state that comprises of horizontal positions and with equal weights of $1/N$. Then, the new state of each particle will be updated based on the last moving information, such as step length, velocity, and direction. The weight of each particle is updated using the measured position from trilateration. Finally, the output position state will be calculated from the updated particles and their weights. Similar to KF, PF is a recursive process. The simulated result in [43] showed that PF is more stable than KF. The RMS error was further decreased from 0.115 m to 0.091 m. The research [94] provided a clearer result to prove that PF is more resistant to jump points. However, PF time consumption (2.4804 s) is significantly higher than KF (0.0156 s), showing a higher computation complexity in PF.

V. SPECIFIC HARDWARE CONFIGURATION FOR LED POSITIONING

The LED positioning systems in surveyed literatures are divided into four (see Figure 13) categories: i) photodiode-based systems, ii) camera-based systems, iii) hybrid systems, and iv) outdoor systems.

A. Photodiode-Based Systems

A photodiode, or photo detector, simply provides a converted current from the incident light. The information that can be exploited from the current is RSS, TDOA, or AOA. Although it provides limited information, the cost of a single photodiode is significantly cheap and it has already been used in most smartphones as a part of their

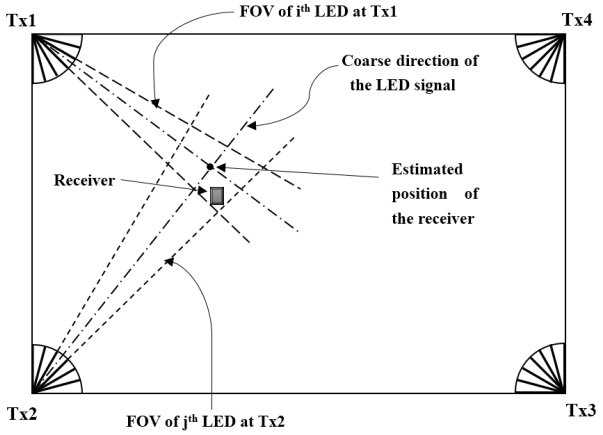

Fig. 14. Multi-element localization system based on AOA [81].

light sensors for brightness auto-adjustment. Furthermore, the CMOS sensor inside a camera is actually a photodiode array. Unfortunately, the photodiodes in these devices cannot be utilized due to the low sampling rate of the optical signal processor which is restricted by software and hardware. Instead, a small light sensor board can be connected to the phone through the audio port, utilizing Analog-to-Digital Converter (ADC) in the audio to sample the signals [33]. With the development of VLC, smart devices will be capable of processing high-rate optical signals in the near future. Many studies have exploited photodiodes to implement indoor positioning. These systems will be discussed separately based on the number of used receivers and transmitters.

1) Single PD, Multiple LEDs: The most typical system of LED indoor positioning uses one PD and multiple LEDs, in which at least three LEDs are needed for the RSS-based positioning system. Furthermore, TDOA-based systems require at least three LEDs for 2D localization, and four LEDs for 3D localization. The AOA-based system is unique (see Figure 14). The receiver is surrounded by multiple transmitters, each consisting of multiple elements [81] which are fan-shaped LED with limited FOVs. Therefore, receiving the signal from a LED implies that the receiver is within its FOV of the LED. The location of the receiver will be roughly determined by two elements from different transmitters. Accuracy can be enhanced by increasing the number of transmitters.

As shown in Figure 15, another specific system, based on single PD and multiple LEDs, used the angular diversity transmitter, which consists of multiple LEDs and a biconvex lens [95]. The LEDs in the transmitter are distinguished by FDM. An illumination pattern forms 25 regions on the floor, then when the target moved into one region, it received signals from a group of LEDs and the location of the receiver was roughly estimated as the center of the region. This approach requires an intensity map of the LEDs. Unlike RSS-based systems, this is a robust solution because it does not need accurate information from the transmitter and receiver (e.g., output power, Lambertian orders, etc.) or noise modelling. However, a large number of transmitters are required to achieve millimeter accuracy.

The idea of separated regions was also found in another IPS system [96]. The difference here is that the transmitter is made

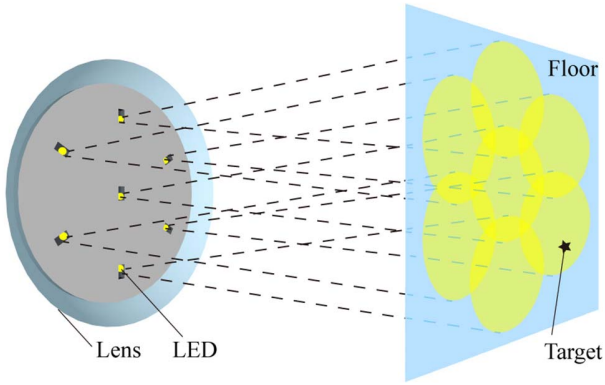

Fig. 15. An example of angular diversity transmitter consisted of 7 LEDs and a biconvex lens. The projected intensity pattern forms 25 regions (7 distinct regions and 18 overlapped regions) on the floor.

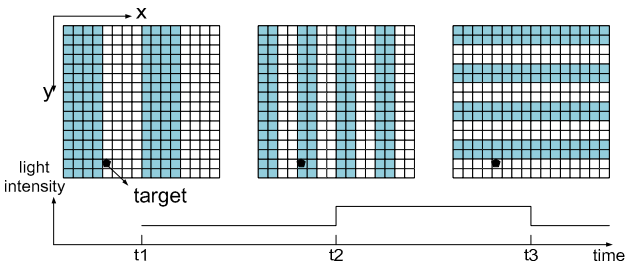

Fig. 16. Top: the light projections of a 16 × 16 LED array on a plane at different times. Bottom: the light intensity received by the target at different times. The update rate of the LED is much faster than the target's moving speed. A unique light intensity sequence of the involved LED (x: 5, y: 15) will be perceived by the optical receiver on the target.

of one complete LED array panel. As depicted in Figure 16, the illumination pattern is the projection of the LED array and the projected regions (pixels) from the 16 × 16 LEDs barely overlap. The idea of using non-overlapping regions to perform positioning may derive from the adoption of a space-division multiple access (SDMA) scheme in VLC. The location of the receiver will be only determined by the connected LED. The system is tested by tracking a moving object in the frame rate of 333 fps. Thus, the object is nearly static in a sequence streaming interval. An error of 1.64 pixels was reported in an 8×8 m^2 plane when the distance is 40 cm [96].

2) Single PD, Single LED: Technically, positioning using a single PD and a single LED is impossible. To deal with this case, the research [33] used inertial sensors to measure the incidence and irradiation angles when the phone was rotated. The idea was that when the phone faced squarely to the light, the measured RSS was at the peak point and the corresponding angle was the incidence angle when the phone was placed horizontally. With this information, the distance could be calculated using the model equation. A compass in the smartphone measured the direction of the phone when it faced the light. Finally, the location was calculated by using the obtained distance and direction. Although this process was complicated and time-consuming, and the performance was about 95% below 1 m, which was much worse than multiple LEDs locating system (90% below 0.45 m), it could be a complementary solution to some harsh situations, especially when the light sources were deficient.

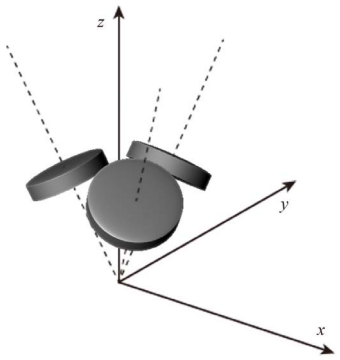

Fig. 17. The structure of multiple tilted optical receivers [46].

3) Multiple PDs, Single LED: Many works have attempted to use multiple photo detectors for single transmitter positioning. A circular plate shaped device was designed with three attached photo detectors in [45]. This 2D localization design exploited RSS values from optical signals in order to calculate the horizontal distances from each receiver to the transmitter. Since the relative position of these three photo detectors was fixed, the rotation angle of the circular device could be determined by minimizing the distance deviation of two receivers when rotating the device around the third receiver. The device was then located in the middle of three receivers.

The study [46] further improved the above design by using three tilted and separated photo detectors, as illustrated in Figure 17, instead of horizontal optical receivers. This new design, called "angular diversity detectors", also assured more stable conditions for MIMO VLC systems [97]. In this design, receivers were close enough so that the distances from each receiver to the transmitter were nearly equal. However, the received signal intensity was different due to the tilted receivers. In the channel model, the received power was related to the incidence angle gain. This research calculated the incidence angle gain difference between every two receivers at each location on the map with unchanged azimuth angle of the receivers. The results turned out to be a hyperbolic cluster for each pair [46]. Finally, the location of the receiver was the intersection point of three lines of incidence angle gain difference. The work [46] reported a positioning error of less than 6 cm in a $2 \times 2 \times 1$ m^3 sized room when the polar angle was 10°, which was caused by imperfectly matched gain profile and fluctuated RSS. The angular diversity receiver was proposed in [98], which utilized 6 PDs to provide a wider receiving angle and which performed better in a challenging environment. The experiment result showed that the system could achieve an average positioning error of 0.4 m in an office environment (24×16 m^2) with only three LED lamps.

The Cramer-Rao Lower Bound (CRLB) for the IPS based on an angular diversity receiver was derived in [99]. A small difference between this work and the aforementioned one [98] was that the receiver consisted of several horizontal elements. Each element had a photodiode and an aperture few millimeters away from the center of the PD to provide angle diversity. The CRLB showed that the centimeter accuracy can be achieved under 1W optical power.

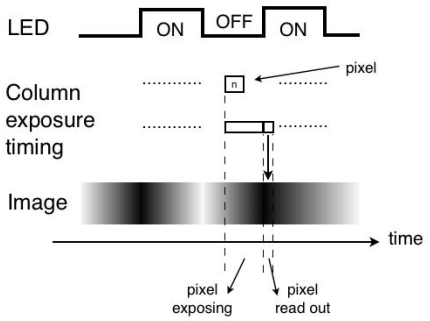

Fig. 18. Rolling shutter effect of a CMOS camera. Pixel n belongs to n^{th} column of the CMOS array [49].

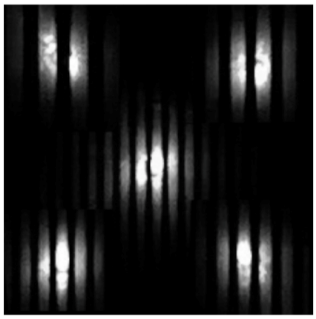

Fig. 19. An image of five LEDs under rolling shutter effect [49].

B. Camera-Based Systems

The camera on the smartphone, also known as the image sensor, can be used for IPS. It takes images of the light beacons successively and feeds them to the positioning software to estimate the location of the receiver. The image provides the locations of the light beacons on the image coordinate. With these locations, AOA information could be retrieved. Thus, AOA is often exploited in camera-based positioning systems. Meanwhile, RSS is never used for this category because the light intensity on the image cannot be accurately measured due to the limitation of the sampling rate. The techniques exploited in camera-based IPSs will be discussed in this section.

1) Rolling Shutter Effect: How to identify each light beacon for better decoding in images is a fundamental process in camera-based IPSs. The kHz-frequency flicker of light, which is imperceptible to humans, can be detected by the camera. Therefore, LED can transmit its identity code by switching frequency like FDM modulation. The camera employs a pixel detection method to determine the ON and OFF status of the light and extract the identity code. In fact, the rolling shutter effect, a technical term in photography, which is widely used in VLC [100]–[102] and visual positioning systems [103], has been exploited for data extraction in images in IPS [49], [104].

The Rolling shutter effect occurs when capturing images with short exposure time. During the exposure, the CMOS sensor in the camera can be saturated for several columns of pixels, but it can only read out one column each scanning time. Consequently, as shown in Figure 18, when the light – modulated by On-off Keying – is OFF, it will not have enough time to saturate a column before the camera scans the column, resulting in a black and white spaced image. This effect will be more obvious when the exposure time is shorter. However, the exposure time should not be too short as the picture would be too dark.

Film speed (ISO setting) is another important camera parameter that determines how many photons are required to light up a pixel. If the intensity of received light is low, the contrast of the image can be enhanced by decreasing the film speed. With rolling shutter effect, the code sequences (i.e., ID, coordinate, or any other information) transmitted by modulated LEDs can be detected using only one image, largely mitigating the computation load of image processing. Although most encoding methods were applicable, a hybrid of pure tones and Manchester encoding was suggested to fit both short and long distance localization systems [49].

As presented in Figure 19, the image decode process works after images are obtained from all the transmitters. The process includes image cropping, Gaussian blurring, binarization processing, and edge detection [49]. In Figure 19, the bright row near the center of each transmitter image is wider and closer to the neighboring row, which means edge detection error is more likely to occur. Therefore, it is important to keep a low speed for the LED switching. In a real-world environment, the band pattern is much more obscure than the presented figure. Moreover, some of the measured light intensity during the "OFF" period might be higher than that during the "ON" period. Thus, the quantization value needs calibration for each column on the image during binarization. The research [104] suggested an approach to precisely determine the quantization value, where the intensity of each bright and dark band was measured and a threshold line was calculated to differentiate ON and OFF states.

2) Double-Camera Localization: Camera-based IPSs need at least azimuth angle information, usually measured by magnetometer, to locate the target. In [78], [105], and [106], a method was proposed to perform positioning without angular measurements. Therefore, the system was free from angular errors. Two identical cameras were used and placed horizontally at the same height in this method. As shown in Figure 20, the optical signals passed through the lens in front of the CMOS sensors and projected onto one point of each sensor respectively. As a result, a pair of two similar triangles Δ_{abc} and Δ_{ade} could be plotted. Known variables were $\overline{bd}$, $\overline{ce}$, $\overline{bc}$, and $\overline{de}$. $\overline{bd}$ and $\overline{ce}$ could be calculated by using the focal length of the sensor and the location of the projection on the image. $\overline{bc}$ was the distance between two centers of the lens. $\overline{de}$ was the distance between the projections on images. In the similar triangles, the proportion relationship of the two triangles could be calculated using $\overline{bc}$ and $\overline{de}$. Then $\overline{ab}$ and $\overline{ac}$ could be acquired. The distance between the LED and the receiver was the median of the triangle Δ_{abc}. Different from the AOA-based localization, this method measured all the distances between the transmitters and the receiver and adopted basic trilateration method to locate the receiver.

3) Single-Camera Fused With Inertial Sensors: The double-camera scheme has the disadvantage of requiring

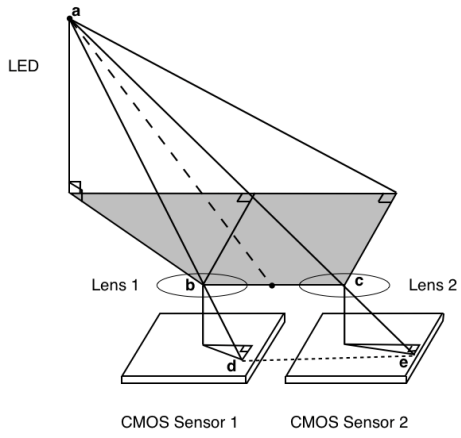

Fig. 20. The positioning technique using two identical cameras.

specific and costly receivers. A single camera scheme is frequently adopted as it utilizes smartphone-embedded modules. The research [107] proposed a smartphone-based positioning system that used a single light source (aiming to mitigate the cost for dense distribution of light sources), single camera, and the inertial sensors (aiming to avoid the influence of rotation). The camera firstly captured the image of the light source and then the inertial sensors measured the rotation matrix to restructure the image. Data transmitted by the light source was retrieved by using the rolling shutter effect. Furthermore, five reference points chosen from the image, mainly from the contour of the light projection, were needed in the positioning. Correspondingly, five equations of geometry relationships were constructed with five AOAs retrieved from the image transformation algorithm. The target position was then obtained by using the Levenberg-Marquardt algorithm. Experiment result showed that 4.96 cm accuracy for 3D localization could be achieved in a $0.7 \times 0.7 \times 1.8$ m^3 test bed.

C. Hybrid Systems

The hybrid positioning system combines VLC positioning with other systems, such as inertial sensors and RF systems [58], [98], [108]–[112]. Currently, hybrid systems are designed to address major problems like inaccurate LED parameters, unstable receiver's attitude, and occlusion between LED and the target.

A hybrid of LED fingerprinting system and an improved spring model based on Bluetooth signal was proposed in [109]. The spring model was especially utilized in the positioning field to perform collaborate adjustments on multiple target locations, which is similar to the balancing process of a spring [113]. When the fingerprinting system failed to locate some of the targets, the spring model could still provide a rough estimate for these targets. In this system, smartphones with Bluetooth function were used as APs and the distances between APs and the target were derived from the Bluetooth propagation model. These distances served as the inputs of the spring model. With these distances and the initial position estimation from LED fingerprinting, the spring model would provide an improved position estimation. Simulations demonstrated that 6 cm accuracy could be obtained with 5 cm grid size of the fingerprint map.

Besides this Bluetooth hybrid system, combination with other RF signals is merely studied. Instead of RF signals, most LED hybrid positioning systems were coupled with inertial sensors [58], [98], [108], [110]–[112].

The work [58] addressed the issue of receiver's attitude in 3D positioning. This system utilized accelerometers to measure attitude of the receiver, providing an accurate angle estimation for photodiode-based AOA triangulation positioning. Another hybrid system fusing camera with inertial sensors was proposed in [112].

The combination of LED positioning and pedestrian dead reckoning (PDR) is an important research method in the hybrid positioning system to improve the positioning accuracy [98], [108], [110]. This combination leverages the advantage of PDR that it can offer accurate short-term tracking. Unfortunately, in long-term, the PDR system will not operate well with large cumulative positioning errors unless it is fused with absolute locations from other systems. The LED-based positioning system can provide absolute positions to centimeter-level accuracy, however, it often suffers from obstacle occlusion and unstable illumination. Therefore, considering their complementary characteristics, LED positioning system and PDR can be fused to achieve a robust positioning system.

The work [110] proposed a hybrid system of camera-based IPS and PDR. When the receiver was covered by the LED lamps, the position of the receiver was estimated using the image transformation method. Otherwise, positions were estimated by PDR. Experiments showed that the maximum error was less than 1 m for a total of 50 m walking inside a building.

The PF algorithm was used to fuse LED and PDR in [98] and [108]. The general process of the system was depicted in Figure 21. Usually, the system model utilized the PDR output while the position acquired from LED positioning served as the measurements. By adopting this process, the work [108] showed the average positioning error have been reduced from 0.34 m in the standalone VLC positioning to 0.14 m in the hybrid system. The research [98] proposed a peak detection method in VLC positioning to ensure that the system can be deployed under non-uniform lighting conditions. It did not require accurate intensity and the location was provided when the receiver was positioned directly under the LED lamp and detects the peak optical intensity. This system was tested in a large-scaled school building and the average error was 0.38 m, which was much less than the 5.8 m of the standalone PDR approach. In [114], the feasibility of fusion of PF and PDR was verified in a large hall way and a significant improvement of accuracy was reported in the experimental result. The accuracy was 0.24 m (90%), which was better than the pure PDR (0.99 m, 90%).

D. Outdoor Systems

The outdoor LED positioning is another aspect of visible light positioning applications. As compared to GPS, the

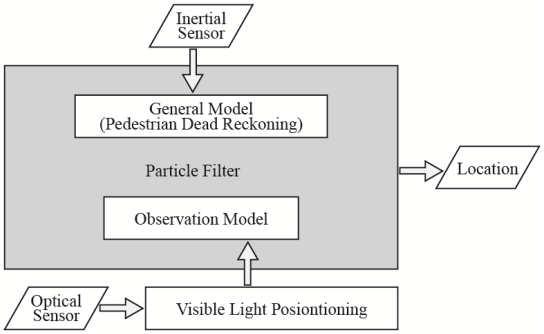

Fig. 21. The general process of PF to fuse PDR and LED in a hybrid positioning system.

main purpose of outdoor LED positioning is to provide vehicles and pedestrians with more accurate navigation service. Although both systems use LEDs as their transmitters, outdoor VLC positioning is much different from current indoor applications. The major difference is the alignment of the lights. Indoor positioning mainly utilizes pre-organized and fixed ceiling lights as the transmitters, whereas for outdoors the main light source could be traffic lights, vehicle headlights/taillights, or street light posts. Consequently, there are many challenges for outdoor applications because many of these lights are either poorly distributed or moving and there is also strong ambient light disturbance. Besides, real-time tracking of fast vehicles is also required for outdoor applications. The main applications of outdoor positioning are discussed as follows.

1) Vehicle to Infrastructure (V2I) Positioning Using Traffic Lights: As a 24-hour signaling device, the LED traffic light can be utilized to continuously provide positioning service for vehicles in its vicinity. LED panels in the traffic light can be modulated to broadcast information like location code to the receiver on the vehicle.

The research [115] involved a 9 partitioned panel that transmitted a location code within a traffic light by way of symbols in a sequence operated by switching various partitions on and off (250Hz update rate). Vehicles used cameras with 50 fps capture rate to capture images from the traffic lights and extracted the code through image processing. The distance between the vehicle and the traffic light was calculated using the similar triangle method involving the actual size of the LED panel, the projected location on the image and the focus length of the lens. However, if a vehicle was moving at 50km/h speed, it would be difficult to distinguish the images and it required at least 500 fps capture rate to successfully extract the code. Under relatively low SNR environment, the work [115] optimized the system by using median filtering, setting thresholds in image processing, and adding colored mask filter to the camera.

The V2I 3D positioning was presented in [31], where the camera captured two traffic lights and one additional LED beacon. Simulation results showed that the positioning error was 7 cm when the resolution of the camera achieved 1000×1000 pixels.

For the research [116], a photodiode-based positioning was designed and the vehicles were equipped with two photodiodes on their front lights. Two different systems were tested, i) using one traffic light and ii) using two lights. For the single-light application, two photodiodes measured the TDOA of the traffic signal, then re-measured it when the vehicle moved to another location, the measurements creating two sets of hyperbola. This resulted in the position of the object staying within the area formed by the crossed points of these hyperbolas. The two-light application involved a vehicle traffic light and a pedestrian traffic light. Each light was modulated in different frequencies while two photodiodes measured the TDOAs simultaneously. Coplanar rotation methods were designed for both applications in order to cope with the error induced by non-coplanar (when vehicles are close to the traffic lights) of the two hyperbolas. The simulation result showed the proposed algorithm enhanced the positioning accuracy to 0.5 m from 10 m when the vehicle was 3 m from the traffic light.

2) Vehicle to Vehicle (V2V) Positioning Using Head/Tail Lights: Vehicles perform LED positioning by transmitting visible light signals to each other through their illuminations. An application is that the rear vehicle uses headlights to transmit the signals while the forward vehicle uses photodiodes to receive them. Current applications mainly adopt TDOA rather than RSS for LED signals, probably due to inconsistent dimming of the lights during driving.

In [117], two headlights of the rear car were tuned to different frequencies and two PDs were attached to the taillights of the forward car to measure TDOAs simultaneously, which were converted to distance deltas by considering the speed of light; thus, the relative distance was easily calculated by using the geometric relationship between two triangles with the same height. The field experiments showed centimeter-level accuracy when given 1 m distance between vehicles.

3) Positioning in Tunnel Environment: LED lights were used for positioning in tunnels where GPS signals were not available. The research [118] designed a VLC-based positioning system by combining V2V and V2I. The camera installed on the vehicle captured the LED signals from the forward car and illumination infrastructure in the tunnel. The system considered OOK modulation for VLC to transmit location data. In order to eliminate unrelated LED sources in the image, the system performed an intensity filtering process before storing the differential images. The three closest LED signals on the image – either the tunnel lights or the car lamps – were used to estimate the 3D location of the car. In this system, collinearity condition and the rotation matrix were considered in coordinate transformation. The accuracy was reported to within 1 m in simulated experiments when the distance from the first LED source was less than 20 m.

4) Positioning in Underground Mines: Positioning in an underground mine can provide assistance for transportation of minerals and emergency navigation during accidents. RF-based positioning systems were studied since radio communication devices were generally installed underground. However, because radio signals are easily affected by the complicated signal disturbance and the bumpy surface of the underground walls, the positioning performance is unsatisfactory. On the other hand, by leveraging illumination infrastructures, it was possible to develop a cost effective and accurate underground positioning system. The research [119] proposed a 1-D

VLC-based positioning system where an OOK modulation was adopted to represent a LED lamp's ID. The signals were received by PD, whose position was estimated using the proximity algorithm. This system was able to switch the positioning accuracy for different applications by controlling the number of activated lights, thus resulting in different signal overlapping situations.

5) Underwater Positioning Using Light Beacons: Underwater positioning is essential for ocean research as it is required to guide autonomous underwater vehicle (AUV) or remotely operated vehicle (ROV) to perform underwater or deep-water surveying. High-accuracy and high-rate positioning is especially required when a ROV is near its target. Thus, optical positioning systems can be a cheap and high-accurate solution.

The research [120] involved tracking a target AUV, which possessed three light beacons to transmit their IDs, by a wide FOV camera on a leader AUV. A fisheye distortion model was used to correct the radial distortion caused by the fisheye camera lens. If three light beacons were captured on the image, it was enough to estimate the target AUV's pose with respect to the camera. The distance between the AUVs was estimated by using the geometry of relative positions of the beacons on the image and the beacon's location on the target AUV. The EKF was utilized to reduce the noise in the pose and distance estimation, in which the position and velocity of the target formed the state vector and the camera measurements contributed to the measurement model. This underwater experiment showed such system could achieve centimeter-level accuracy.

VI. Performance Analysis of LED IPSs

In this section, the LED-based IPSs will be reviewed and compared under the criteria of accuracy, complexity, cost, and commercial availability. The details will be presented in the form of two tables based on the type of receiver: Table IV–photodiode-based IPSs and Table V–camera-based IPSs. Due to the large number of photodiode-based designs surveyed in this article, we organize them in the priority of, i) their signal characteristics – RSS, TDOA, and AOA, and ii) the algorithms employed. Please note that H_{re} in these two tables represents the receiver's height above the ground.

A. Accuracy

The accuracy, or localization error, of each system is presented in the tables. Prior to the analysis, it should be noted that the size and difficulties posed in the test environment for each system are very different; thus, there should be a downscale of the accuracy for each system before the comparison can be made. Apart from the size of the test area, the test mode should also be considered in the analysis of accuracy, i.e., whether it is experimental or simulation, whether the dimensions are 2D or 3D, and whether there is noise. Generally, simulation results are better than experimental results, and 2D localization has a lower positioning error than 3D localization.

As shown in TABLE IV, only RSS and AOA based designs have been tested in real positioning conditions. So far, there is no experiment result for TDOA-based IPS, the feasibility of this positioning technique is unknown. Based on the experimental results, RSS-based systems and AOA-based systems show almost the same performance in positioning accuracy [33], [52], [58], [111]. The result also shows that AOA positioning are more accurate in PD based designs than in camera based designs [52], [58], [124]. Among the systems that apply the same technique, the trilateration algorithm has achieved the highest accuracy, while proximity has achieved the lowest. To some extent, filtering algorithms improve the positioning accuracy. It is found that those systems modulating LEDs with the TDM multiplexing protocol perform more poorly than those modulated by FDM, due to the impact of the synchronization error. Finally, it is found that the camera-based system is usually more accurate if an auxiliary device is utilized.

B. Complexity

The complexity of these systems is assessed based on both their design and implementation complexities. It is found that proximity is the fastest method among all the positioning algorithms. The process time of fingerprinting depends on the size of the search area of the fingerprints in the database. Trilateration, triangulation, and multilateration need geometric analysis, which includes distance or angle calculation and the application of estimation algorithms, hence, they are more complex. Filtering, based on probability theory, is found to be the most sophisticated method. Furthermore, it is noticeable that using inertial sensors decreases the complexity of LED positioning algorithms. On the other hand, the use of inertial sensors introduces extra steps for processing the inertial data. Implementation complexity also depends on the number of used LEDs and the need of extra hardware or database. AOA-based IPSs can be realized simply by the smartphone's build-in camera, while TDOA and RSS based systems require attached prototype hardware.

C. Cost

The implementation cost refers not only to the expense of the devices, but also to the time spent on deploying a whole system. An advantage of IPS using LED lights is that the existing LED infrastructures in the buildings would be sufficient to save both time and money. The LEDs are very long lasting and energy efficient, thus they incur very low costs for maintenance. Dense distribution of lights in some IPS designs might incur more expense on the transmitters. Considering that LEDs are required to transmit their unique IDs, the cost of circuits connected to the LEDs is inevitable. In spite of this, the overall used wattage is still low. Of all the IPSs, camera-based designs benefit users from avoiding extra expense on the receivers while photodiode-based designs require extra cost on the hardware. Among all the positioning algorithms, proximity and trilateration can be directly used in real-time positioning, and can be quickly deployed. However, on the other hand, fingerprinting is quite time-consuming and labor-intensive since it requires data collection at the offline training stage. In large buildings, where IPSs are mostly required, hours or even days, of training may be needed, especially to achieve high accuracy

TABLE IV
PHOTODIODE-BASED LED IPS SOLUTIONS

System	Positioning Algorithm	Experiment/ Simulation	Testbed Size	Accuracy	LED Parameters	Auxiliary Devices	Consideration of Noise	Cost
[33]	RSS, a: Trilateration b: Modeling	Experiment	a: 5×8, 2×12, 3.5×6.5m b: 3.5×6.5m	a: 30cm b: 110cm 2D	a: 4 LEDs (10W, FDM) b: 1 LED	Inertial Sensor	N	Low
[54]	RSS, Trilateration	Simulation	6×4×4m H_{re}: 1m	< 20cm 2D	4 LEDs (16W, TDM)	N	Y	Low
[48]	RSS, Trilateration	Simulation	1.5×1.5×2m H_{re}: 0.9m	< 3cm 2D	3 LEDs (FDM)	N	N	Low
[40]	RSS, Trilateration	Experiment	0.6×0.6×0.6m	2.4cm 3D	3 LEDs (FDM)	N	N	Low
[43]	RSS, Trilateration + Filters	Simulation	6×6×4.2m H_{re}: 1m	< 15cm 2D	3 LEDs (TDM)	N	Y	Medium
[121]	RSS, Trilateration	Simulation	0.9×0.9×1.5m	1.58cm 2D	3 LEDs (TDM)	N	Y	Low
[111]	RSS, Trilateration	Experiment	Large	0.3~0.44cm 3D	1 LED	Magnetic sensors, 5 extra PDs	Y	Medium
[108]	RSS, Trilateration + PDR + Filters	Experiment	2.5×2.84×2.5m	0.14m 2D	7 LEDs (17W, CDM)	Inertial sensor	Y	Medium
[82]	RSS, Filters	Simulation	Large	High	N LEDs	N	Y	Medium
[66]	RSS, Fingerprinting	Experiment	1.8×1.2×1m step length: 10cm	14.84cm 2D	6 LEDs (FDM)	4 extra PDs	Y	High
[47]	RSS, Fingerprinting	Simulation	6×6×4m	9.1~26.4cm 2D	4 LEDs (10W, FDM)	N	N	High
[71]	RSS, Fingerprinting (Probabilistic)	Simulation	30×30m unit: 1m	0.81m 2D	137 LEDs	N	Y	High
[109]	RSS, Fingerprinting + Spring (Bluetooth)	Simulation	5×3×3m unit: 5cm	6cm 2D	4 LEDs	6 Bluetooth APs	N	High
[72]	RSS, Proximity	Simulation	10×2.5×3m	< 130cm 2D	N LEDs (3W)	N	Y	Low
[122]	RSS, Modeling	Experiment	5×4×3m	60cm	3 LEDs (TDM)	Accelerometer, 3 extra PDs	Y	Medium
[123]	RSS Modeling	Simulation	20×20×3m	3cm 2D	9 LEDs (TDM)	N	N	High
[18]	TDOA, Trilateration	Simulation	5×5×3m	0.18cm 2D	3 LEDs (FDM)	N	N	Low
[16]	TDOA, Trilateration	Simulation	5×5×3m	0.002cm 3D	5 LEDs (FDM)	N	N	Low
[77]	TDOA, Multilateration	Simulation	5×5×3m	3.59cm 3D	9 LEDs (TDM)	N	Y	Low
[76]	TDOA, Multilateration	Simulation	5×5×3m	31.3cm 3D	16 LEDs	N	Y	Low
[58]	AOA, Triangulation	Experiment	5×3×3m	25cm 3D	3 LEDs (TDM)	Accelerometer	Y	Medium
[81]	AOA, Triangulation	Simulation	4×6m	< 15cm 2D	4 LEDs (TDM)	N	N	Low
[52]	AOA, Triangulation	Experiment	5×1×1.5m	29.8cm 2D	1 LED	Inertial sensor	Y	Low
[38]	AOA, Triangulation	Simulation	4×4×3.5m H_{re}: 1m	13.95cm 2D	16 LEDs (TDM)	Inertial Sensor	Y	Low
[96]	AOA, Coverage	Experiment	8×8×40cm	8.2mm 2D	16×16 LED array (SDM)	Aspherical lens on LED	Y	High
[95]	AOA, Coverage	Simulation	5×3×3m H_{re}: 1m	12.9cm 2D	9 LEDs (7 units, FDM)	Biconvex lens on LED	Y	High

to within a few centimeters. Moreover, if the locations of some light anchors have to be changed, a huge volume of database material needs to be updated.

D. Commercial Availability

In order to analyze the commercial availability of a design, it is necessary to globally consider the accuracy, complexity and

TABLE V
CAMERA-BASED LED IPS SOLUTIONS

System	Positioning Algorithm	Experiment/ Simulation	Testbed Size	Accuracy	LED Parameters	Auxiliary Devices	Consideration of Noise	Cost
[82]	AOA, Transformation	Simulation	Large	High	N LEDs	N	N	Low
[78]	AOA, Transformation	Experiment	0.6×0.6×2.6m	6.1cm 3D	2 LEDs	One Extra Camera	N	Medium
[124]	AOA, Transformation	Experiment	6×6×4m H_{re}: 1.5m	< 40cm 2D	9 LEDs	N	Y	Low
[106]	AOA, Trilateration	Simulation	1.8×1.8×3.5m	15.6cm 3D	4 LEDs	One Extra Camera	N	Medium
[107]	Transformation	Experiment	0.7×0.7×1.8m	1.5cm 2D 2.67cm 3D	1 LED (5W)	Gyroscope	Y	Low
[49]	AOA, Triangulation	Experiment	0.71×0.74×2.26 m	10cm 3D	5 LEDs (FDM)	N	N	Low
[125]	Transformation	Experiment	1.4×1.4×1.6m	X: 3cm Y: 7cm	3 LEDs (CDM)	N	Y	Low
[110]	Transformation + PDR	Experiment	50m walking distance	< 1m 2D	NA	Inertial sensor	Y	Medium
[112]	Transformation	Experiment	1.8m	4.3cm 3D	3 LEDs (10W, CDM)	Inertial sensor	Y	Low

cost – the first priority being the cost. The commercialization is easier when smartphones and the existing infrastructures can be leveraged. Navigation applications can be quickly developed and pushed towards the market if the smartphone can act as the receiver. Therefore, camera-based designs are more likely to be acceptable for the LED IPS. However, the camera is a power-consuming module on the smartphone and it is perpetually running during its positioning phase. Thus, a power-saving method should be explored for camera-based designs.

The RSS-based and AOA-based VLC positioning systems have been experimentally validated. The possibility of commercializing these techniques relies on designing smaller and cheaper hardware for more widespread use in smart devices. The TDOA-based system shows potential in accurate positioning based on simulation results. However, it has the problem of requiring an extra photodiode as the receiver. This requirement limits its application. Furthermore, this technique requires validation in real-world experiments. Proximity and trilateration methods could be easily commercialized in indoor environments. If the distribution of illumination is dense and centimeter-level accuracy is not required, deploying proximity is the better choice. Otherwise, trilateration is a more suitable solution. For the fingerprinting technique, even though it is favored in commercialized WiFi positioning applications, the situation is different in LED IPS, as the demand of centimeter-resolution of fingerprints obviously increases the cost. This method requires further investigation.

VII. CHALLENGES AND POSSIBILITIES OF LED IPSS

Research so far has explored many possibilities in the design of LED positioning techniques, as well as various traits of the LED IPSs. Much consideration has been given to the inevitable noise and errors in the applications. Whereas, there are still many open issues in this field, in this section we would like to express our principle concerns and make some suggestions for future research.

Visible light positioning performance will be improved following the development and roll-out of VLC systems, which are capable of achieving high data rates. In the IPS design, it is important that the modulated bandwidth of the lights should not hold back the implementation of a VLC system. Hence, how to expand the optical channel bandwidth is a meaningful topic to warrant further research. However, high data rates transmitted by the lights make data decoding more difficult for optical sensors, also deemed as one of the main challenges in VLC.

With regard to positioning applications using multiple light sources, the capabilities of TDM and FDM, along with other specific multiplexing protocols in VLC, such as code division multiple access (CDMA), single carrier frequency division multiple access (SC-FDMA) [126], and non-orthogonal multiple access (NOMA) [127], need further study and validation to ensure fast and reliable data transmission over the shared medium. Furthermore, an appropriate choice of bandwidth for FDM protocols should be explored. More encoding schemes adopted by VLC technology need to be verified in LED positioning. Also, LED IPS research may be largely promoted if a standard circuit for LED controlling is designed to mitigate the works for experiment deployment.

Since it is difficult to deploy RSS-based IPSs as smartphone applications, discovering more convenience for smartphone users is a very valuable area for commercializing LED positioning. However, a more standard receiver may be specified for LED positioning instead of smartphones. The influence of anchor density on the localization performance has not yet been seriously evaluated. In addition, multipath effect, interference among the anchors, and noise from the environment need further investigation in respect of LED IPS; hence, a more precise optical channel model should be designed and verified based on these factors. In order to foster the self-adapting ability in the dynamic environment it is recommended that channel training should be performed every time the positioning application starts. Moreover, it is suggested that all designed IPSs should be experimentally tested, especially in

large-scale and complex environments, such as in hallways and corridors, in order to evaluate their tolerance to noise and errors. In particular, TDOA-based positioning systems should be put into practice and experimental results are expected to verify their feasibility.

Most RSS-based research has reported a relatively low accuracy of positioning on the edges, or corners, of the experimental environment. However, the solution to this kind of problem has not yet been explored in LED positioning. Another concern is that, even though the fact that the visible light signals that cannot penetrate walls, there might be an interfering situation at the door or when a glass wall exists between rooms. Localization in such cases still presents a challenge for the commercialization of LED positioning systems. A further problem is that positioning performance may degrade during daytime, when the lights are off, or only partly switched on. Thus, a complementary positioning system, such as inertial sensors, WiFi, Bluetooth, infrared lights, or Ultra Wide Band (UWB), should be utilized.

In particular, millimeter wave (mm-wave) communication has been recognized as a promising technology enabling high data rate transmission for future fifth generation (5G) communication networks, since there are huge, unlicensed spectrum bands available at mm-wave frequencies in the range of 30-300 GHz [128]. For instance, Samsung Electronics announced in 2014 the development of 60 GHz WiFi technology based on the IEEE 802.11ad standard [129], which achieved data transmission speeds of up to 4.6 Gbps, more than ten times faster than that of 2.4 GHz and 5 GHz WiFi technologies [130]. As a result, it will be a trend to place mm-wave access points in future indoor environment to meet the increasingly high data rate demand. Different from the microwave transmission, mm-wave transmission has some similar features as VLC, such as directional transmission and sparse channel model [128], due to the very short wavelength. Thus, in order to reduce the complexity, mm-wave communication systems usually employ offline designed analog beam codebooks, where a cell coverage can be divided into multiple spatially orthogonal beam sectors by the shaped beam patterns in beam codebooks [130]–[132]. In this case, it will be easy to determine the angular range for a terminal by beam training. Therefore, mm-wave IPS will also play an important role in future localization [133], [134]. It would be very interesting to study the hybrid IPS based on mm-wave systems and LEDs. Finally, it is also important to verify the positioning accuracy and robustness of the integration system when using different positioning techniques.

VIII. Conclusion

This article presented a detailed survey of LED positioning systems and critically reviewed the whole system step by step. Many application scenarios were listed to show the requirements and possibilities of indoor localization using LEDs. Then the major features of LED positioning systems were thoroughly discussed, including the channel model, multiplexing protocols, FOV, noise, multipath, and errors. Conclusions from related studies were presented with a view to assist investigators to better understand IPS designs and to aid further comprehensive researches. The article also discussed LED positioning algorithms, which had been expounded in literature in the following categories: RSS, TOA/TDOA, and AOA. The surveyed LED positioning systems were classified into, i) photodiode-based systems, ii) camera-based systems, iii) hybrid systems, and iv) outdoor systems, and all the related techniques were discussed in detail. This article was the first one to survey and classify outdoor applications of LED positioning systems. Furthermore, this article analyzed the conditions and performances of these positioning systems and made comparisons based on such crucial factors as accuracy, complexity, cost, and commercial availability. Next this article surveyed open issues, challenges, and future research directions in VLC positioning systems. Finally, we hope and expect that this article will promote the development of more accurate and robust LED positioning systems.

References

[1] E. D. Kaplan and C. J. Hegarty, *Understanding GPS: Principles and Applications*. Boston, MA, USA: Artech House, 2006.

[2] H. Lan, C. Yu, Y. Zhuang, Y. Li, and N. El-Sheimy, "A novel Kalman filter with state constraint approach for the integration of multiple pedestrian navigation systems," *Micromachines*, vol. 6, no. 7, pp. 926–952, 2015.

[3] Y. Zhuang and N. El-Sheimy, "Tightly-coupled integration of WiFi and MEMS sensors on handheld devices for indoor pedestrian navigation," *IEEE Sensors J.*, vol. 16, no. 1, pp. 224–234, Jan. 2016.

[4] Y. Zhuang, Z. Syed, Y. Li, and N. El-Sheimy, "Evaluation of two WiFi positioning systems based on autonomous crowdsourcing of handheld devices for indoor navigation," *IEEE Trans. Mobile Comput.*, vol. 15, no. 8, pp. 1982–1995, Aug. 2016.

[5] P. Bahl and V. N. Padmanabhan, "RADAR: An in-building RF-based user location and tracking system," in *Proc. 19th Annu. Joint Conf. IEEE Comput. Commun. Soc. (INFOCOM)*, vol. 2. Tel Aviv, Israel, 2000, pp. 775–784.

[6] A. K. M. M. Hossain and S. Wee-Seng, "A comprehensive study of Bluetooth signal parameters for localization," in *Proc. IEEE 18th Int. Symp. Pers. Indoor Mobile Radio Commun. (PIMRC)*, Athens, Greece, 2007, pp. 1–5.

[7] Y. Zhuang, J. Yang, Y. Li, L. Qi, and N. El-Sheimy, "Smartphone-based indoor localization with Bluetooth low energy beacons," *Sensors*, vol. 16, no. 5, 2016, Art. no. E596.

[8] A. R. J. Ruiz, F. S. Granja, J. C. P. Honorato, and J. I. G. Rosas, "Accurate pedestrian indoor navigation by tightly coupling foot-mounted IMU and RFID measurements," *IEEE Trans. Instrum. Meas.*, vol. 61, no. 1, pp. 178–189, Jan. 2012.

[9] Y. Po and W. Wenyan, "Efficient particle filter localization algorithm in dense passive RFID tag environment," *IEEE Trans. Ind. Electron.*, vol. 61, no. 10, pp. 5641–5651, Oct. 2014.

[10] S.-H. Fang, C.-H. Wang, T.-Y. Huang, C.-H. Yang, and Y.-S. Chen, "An enhanced ZigBee indoor positioning system with an ensemble approach," *IEEE Commun. Lett.*, vol. 16, no. 4, pp. 564–567, Apr. 2012.

[11] H. Haas, L. Yin, Y. Wang, and C. Chen, "What is LiFi?" *J. Lightw. Technol.*, vol. 34, no. 6, pp. 1533–1544, Mar. 15, 2016.

[12] D. Karunatilaka, F. Zafar, V. Kalavally, and R. Parthiban, "LED based indoor visible light communications: State of the art," *IEEE Commun. Surveys Tuts.*, vol. 17, no. 3, pp. 1649–1678, 3rd Quart., 2015.

[13] A. Sevincer, A. Bhattarai, M. Bilgi, M. Yuksel, and N. Pala, "LIGHTNETs: Smart lighting and mobile optical wireless networks—A survey," *IEEE Commun. Surveys Tuts.*, vol. 15, no. 4, pp. 1620–1641, 4th Quart., 2013.

[14] P. H. Pathak, X. Feng, P. Hu, and P. Mohapatra, "Visible light communication, networking, and sensing: A survey, potential and challenges," *IEEE Commun. Surveys Tuts.*, vol. 17, no. 4, pp. 2047–2077, 4th Quart., 2015.

[15] N. U. Hassan, A. Naeem, M. A. Pasha, T. Jadoon, and C. Yuen, "Indoor positioning using visible LED lights: A survey," *ACM Comput. Surveys*, vol. 48, no. 2, pp. 1–32, 2015.

[16] U. Nadeem, N. U. Hassan, M. A. Pasha, and C. Yuen, "Highly accurate 3D wireless indoor positioning system using white LED lights," *Electron. Lett.*, vol. 50, no. 11, pp. 828–830, 2014.

[17] Z. Zhou, M. Kavehrad, and P. Deng, "Indoor positioning algorithm using light-emitting diode visible light communications," *Opt. Eng.*, vol. 51, no. 8, pp. 1–6, 2012.

[18] S.-Y. Jung, S. Hann, and C.-S. Park, "TDOA-based optical wireless indoor localization using LED ceiling lamps," *IEEE Trans. Consum. Electron.*, vol. 57, no. 4, pp. 1592–1597, Nov. 2011.

[19] *Visible Light Beacon System*, JEITA, Japan, 2013.

[20] *Visible Light ID System*, JEITA, Japan, 2007.

[21] S. Rajagopal, R. D. Roberts, and S.-K. Lim, "IEEE 802.15.7 visible light communication: Modulation schemes and dimming support," *IEEE Commun. Mag.*, vol. 50, no. 3, pp. 72–82, Mar. 2012.

[22] M. A. Khalighi and M. Uysal, "Survey on free space optical communication: A communication theory perspective," *IEEE Commun. Surveys Tuts.*, vol. 16, no. 4, pp. 2231–2258, 4th Quart., 2014.

[23] W. Zhang and M. Kavehrad, "Comparison of VLC-based indoor positioning techniques," in *Proc. SPIE*, San Francisco, CA, USA, 2013, Art. no. 86450M.

[24] T.-H. Do and M. Yoo, "An in-depth survey of visible light communication based positioning systems," *Sensors*, vol. 16, no. 5, 2016, Art. no. E678.

[25] J. Luo, L. Fan, and H. Li, "Indoor positioning systems based on visible light communication: State of the art," *IEEE Commun. Surveys Tuts.*, vol. 19, no. 4, pp. 2871–2893, 4th Quart., 2017.

[26] Philips. (2015). *Carrefour in France Installs Philips LED-Based Indoor Positioning System*. [Online]. Available: http://www.lighting.philips.com/main/cases/cases/food-and-large-retailers/carrefour-lille.html

[27] Acuity Brands. (2015). *ByteLight™ Services: Indoor Positioning System*. [Online]. Available: http://www.acuitybrands.com/solutions/services/bytelight-services-indoor-positioning

[28] A. Jovicic, "Qualcomm® Lumicast™: A high accuracy indoor positioning system based on visible light communication," San Diego, CA, USA, Qualcomm, White Paper, Apr. 2016.

[29] Y. Zhuang, Z. Syed, J. Georgy, and N. El-Sheimy, "Autonomous smartphone-based WiFi positioning system by using access points localization and crowdsourcing," *Pervasive Mobile Comput.*, vol. 18, pp. 118–136, Apr. 2015.

[30] V. Renaudin, O. Yalak, P. Tomé, and B. Merminod, "Indoor navigation of emergency agents," *Eur. J. Navigation*, vol. 5, no. 3, pp. 36–45, 2007.

[31] M. Yoshino, S. Haruyama, and M. Nakagawa, "High-accuracy positioning system using visible LED lights and image sensor," in *Proc. IEEE Radio Wireless Symp.*, Orlando, FL, USA, 2008, pp. 439–442.

[32] G. Cossu *et al.*, "A visible light localization aided optical wireless system," in *Proc. GLOBECOM Workshops*, 2011, pp. 802–807.

[33] L. Li, P. Hu, C. Peng, G. Shen, and F. Zhao, "Epsilon: A visible light based positioning system," in *Proc. 11th USENIX Symp. Netw. Syst. Design Implement. (NSDI)*, Seattle, WA, USA, 2014, pp. 331–343.

[34] D. C. O. Brien *et al.*, "Visible light communications: Challenges and possibilities," in *Proc. IEEE 19th Int. Symp. Pers. Indoor Mobile Radio Commun.*, Cannes, France, 2008, pp. 1–5.

[35] H. L. Minh *et al.*, "80 Mbit/s visible light communications using pre-equalized white LED," in *Proc. 34th Eur. Conf. Opt. Commun.*, Brussels, Belgium, 2008, pp. 1–2.

[36] H. L. Minh *et al.*, "High-speed visible light communications using multiple-resonant equalization," *IEEE Photon. Technol. Lett.*, vol. 20, no. 14, pp. 1243–1245, Jul. 15, 2008.

[37] L. Zeng *et al.*, "Improvement of date rate by using equalization in an indoor visible light communication system," in *Proc. 4th IEEE Int. Conf. Circuits Syst. Commun. (ICCSC)*, Shanghai, China, 2008, pp. 678–682.

[38] G. B. Prince and T. D. C. Little, "A two phase hybrid RSS/AoA algorithm for indoor device localization using visible light," in *Proc. IEEE Glob. Commun. Conf. (GLOBECOM)*, Anaheim, CA, USA, 2012, pp. 3347–3352.

[39] J. R. Barry and D. G. Messerschmitt, *Wireless Infrared Communications*, vol. 85, New York, NY, USA: Springer, 1994, pp. 265–298.

[40] H.-S. Kim, D.-R. Kim, S.-H. Yang, Y.-H. Son, and S.-K. Han, "An indoor visible light communication positioning system using a RF carrier allocation technique," *J. Lightw. Technol.*, vol. 31, no. 1, pp. 134–144, Jan. 1, 2013.

[41] T. Komine and M. Nakagawa, "Fundamental analysis for visible-light communication system using LED lights," *IEEE Trans. Consum. Electron.*, vol. 50, no. 1, pp. 100–107, Feb. 2004.

[42] M. F. Keskin, E. Gonendik, and S. Gezici, "Improved lower bounds for ranging in synchronous visible light positioning systems," *J. Lightw. Technol.*, vol. 34, no. 23, pp. 5496–5504, Dec. 1, 2016.

[43] W. Gu, W. Zhang, M. Kavehrad, and L. Feng, "Three-dimensional light positioning algorithm with filtering techniques for indoor environments," *Opt. Eng.*, vol. 53, no. 10, 2014, Art. no. 107107.

[44] X. Zhang, J. Duan, Y. Fu, and A. Shi, "Theoretical accuracy analysis of indoor visible light communication positioning system based on received signal strength indicator," *J. Lightw. Technol.*, vol. 32, no. 21, pp. 4180–4186, Nov. 1, 2014.

[45] S.-H. Yang, E.-M. Jung, and S.-K. Han, "Indoor location estimation based on LED visible light communication using multiple optical receivers," *IEEE Commun. Lett.*, vol. 17, no. 9, pp. 1834–1837, Sep. 2013.

[46] S.-H. Yang, H.-S. Kim, Y.-H. Son, and S.-K. Han, "Three-dimensional visible light indoor localization using AOA and RSS with multiple optical receivers," *J. Lightw. Technol.*, vol. 32, no. 14, pp. 2480–2485, Jul. 15, 2014.

[47] U. Nadeem, N. U. Hassan, M. A. Pasha, and C. Yuen, "Indoor positioning system designs using visible LED lights: Performance comparison of TDM and FDM protocols," *Electron. Lett.*, vol. 51, no. 1, pp. 72–74, Jan. 2015.

[48] S.-H. Yang *et al.*, "Indoor three-dimensional location estimation based on LED visible light communication," *Electron. Lett.*, vol. 49, no. 1, pp. 54–56, Jan. 2013.

[49] Y.-S. Kuo, P. Pannuto, K.-J. Hsiao, and P. Dutta, "Luxapose: Indoor positioning with mobile phones and visible light," presented at the 20th Annu. Int. Conf. Mobile Comput. Netw., Maui, HI, USA, 2014, pp. 447–458.

[50] W. Zhang and M. Kavehrad, "A 2-D indoor localization system based on visible light LED," in *Proc. IEEE Photon. Soc. Summer Topical Meeting Series*, Seattle, WA, USA, 2012, pp. 80–81.

[51] N. Kumar and N. R. Lourenco, "Led-based visible light communication system: A brief survey and investigation," *J. Eng. Appl. Sci.*, vol. 5, no. 4, pp. 296–307, 2010.

[52] C. Sertthin, E. Tsuji, M. Nakagawa, S. Kuwano, and K. Watanabe, "A switching estimated receiver position scheme for visible light based indoor positioning system," in *Proc. 4th Int. Symp. Wireless Pervasive Comput. (ISWPC)*, Melbourne, VIC, Australia, 2009, pp. 1–5.

[53] A. Arafa, X. Jin, M. H. Bergen, R. Klukas, and J. F. Holzman, "Characterization of image receivers for optical wireless location technology," *IEEE Photon. Technol. Lett.*, vol. 27, no. 18, pp. 1923–1926, Sep. 15, 2015.

[54] W. Zhang, M. I. S. Chowdhury, and M. Kavehrad, "Asynchronous indoor positioning system based on visible light communications," *Opt. Eng.*, vol. 53, no. 4, 2014, Art. no. 045105.

[55] A. J. C. Moreira, R. T. Valadas, and A. M. de Oliveira Duarte, "Optical interference produced by artificial light," *Wireless Netw.*, vol. 3, no. 2, pp. 131–140, 1997.

[56] J. P. Ding and Y. F. Ji, "Evolutionary algorithm-based optimisation of the signal-to-noise ratio for indoor visible-light communication utilising white light-emitting diode," *IET Optoelectron.*, vol. 6, no. 6, pp. 307–317, Dec. 2012.

[57] T. Q. Wang, Y. A. Sekercioglu, A. Neild, and J. Armstrong, "Position accuracy of time-of-arrival based ranging using visible light with application in indoor localization systems," *J. Lightw. Technol.*, vol. 31, no. 20, pp. 3302–3308, Oct. 15, 2013.

[58] M. Yasir, S.-W. Ho, and B. N. Vellambi, "Indoor positioning system using visible light and accelerometer," *J. Lightw. Technol.*, vol. 32, no. 19, pp. 3306–3316, Oct. 1, 2014.

[59] K. Lee, H. Park, and J. R. Barry, "Indoor channel characteristics for visible light communications," *IEEE Commun. Lett.*, vol. 15, no. 2, pp. 217–219, Feb. 2011.

[60] W. Gu, M. Aminikashani, P. Deng, and M. Kavehrad, "Impact of multipath reflections on the performance of indoor visible light positioning systems," *J. Lightw. Technol.*, vol. 34, no. 10, pp. 2578–2587, May 15, 2016.

[61] W. Gu, M. A. Kashani, and M. Kavehrad, "Multipath reflections analysis on indoor visible light positioning system," *Comput. Sci.*, vol. 57, no. 1, pp. 13–24, 2015.

[62] N. A. Mohammed and M. A. Elkarim, "Exploring the effect of diffuse reflection on indoor localization systems based on RSSI-VLC," *Opt. Exp.*, vol. 23, no. 16, pp. 20297–20313, 2015.

[63] X. Sun, J. Duan, Y. Zou, and A. Shi, "Impact of multipath effects on theoretical accuracy of TOA-based indoor VLC positioning system," *Photon. Res.*, vol. 3, no. 6, pp. 296–299, 2015.

[64] Y. Qi, *Wireless Geolocation in a Non-Line-of-Sight Environment*, Princeton Univ., Princeton, NJ, USA, 2003.

[65] V. Honkavirta, T. Perala, S. Ali-Loytty, and R. Piche, "A comparative survey of WLAN location fingerprinting methods," in *Proc. 6th Workshop Position. Navig. Commun. (WPNC)*, Hannover, Germany, 2009, pp. 243–251.

[66] J. Vongkulbhisal, B. Chantaramolee, Y. Zhao, and W. S. Mohammed, "A fingerprinting-based indoor localization system using intensity modulation of light emitting diodes," *Microw. Opt. Technol. Lett.*, vol. 54, no. 5, pp. 1218–1227, 2012.

[67] M. Youssef and A. Agrawala, "The Horus WLAN location determination system," presented at the 3rd Int. Conf. Mobile Syst. Appl. Services, Seattle, WA, USA, 2005, pp. 205–218.

[68] A. Kushki, K. N. Plataniotis, A. N. Venetsanopoulos, and C. S. Regazzoni, "Radio map fusion for indoor positioning in wireless local area networks," in *Proc. 7th Int. Conf. Inf. Fusion*, Philadelphia, PA, USA, 2005, p. 8.

[69] A. M. Vegni and M. Biagi, "An indoor localization algorithm in a small-cell LED-based lighting system," in *Proc. Int. Conf. Indoor Position. Indoor Navig. (IPIN)*, Sydney, NSW, Australia, 2012, pp. 1–7.

[70] X. Guo, S. Shao, N. Ansari, and A. Khreishah, "Indoor localization using visible light via fusion of multiple classifiers," *IEEE Photon. J.*, to be published.

[71] G. Kail, P. Maechler, N. Preyss, and A. Burg, "Robust asynchronous indoor localization using LED lighting," in *Proc. IEEE Int. Conf. Acoust. Speech Signal Process. (ICASSP)*, Florence, Italy, 2014, pp. 1866–1870.

[72] P. Lou, H. Zhang, X. Zhang, M. Yao, and Z. Xu, "Fundamental analysis for indoor visible light positioning system," in *Proc. 1st IEEE Int. Conf. Commun. China Workshops (ICCC)*, Bejing, China, 2012, pp. 59–63.

[73] Z. Yuxin *et al.*, "Particle filtering for positioning based on proximity reports," in *Proc. 18th Int. Conf. Inf. Fusion (Fusion)*, 2015, pp. 1046–1052.

[74] Y. Zhao *et al.*, "Proximity report triggering threshold optimization for network-based indoor positioning," in *Proc. 18th Int. Conf. Inf. Fusion (Fusion)*, Washington, DC, USA, 2015, pp. 1061–1069.

[75] A. Leick, *GPS Satellite Surveying*. Hoboken, NJ, USA: Wiley, 2004.

[76] A. Taparugssanagorn, S. Siwamogsatham, and C. Pomalaza-Raez, "A hexagonal coverage LED-ID indoor positioning based on TDOA with extended Kalman filter," in *Proc. IEEE 37th Annu. Comput. Softw. Appl. Conf. (COMPSAC)*, Kyoto, Japan, 2013, pp. 742–747.

[77] T.-H. Do, J. Hwang, and M. Yoo, "TDoA based indoor visible light positioning systems," in *Proc. 5th Int. Conf. Ubiquitous Future Netw. (ICUFN)*, Da Nang, Vietnam, 2013, pp. 456–458.

[78] M.-G. Moon, S.-I. Choi, J. Park, and J. Y. Kim, "Indoor positioning system using LED lights and a dual image sensor," *J. Opt. Soc. Korea*, vol. 19, no. 6, pp. 586–591, Dec. 2015.

[79] Y. Li *et al.*, "Self-contained indoor pedestrian navigation using smartphone sensors and magnetic features," *IEEE Sensors J.*, vol. 16, no. 19, pp. 7173–7182, Oct. 2016.

[80] P. Aggarwal, Z. Syed, and N. El-Sheimy, *MEMS-Based Integrated Navigation*. Boston, MA, USA: Artech House, 2010.

[81] Y. S. Erogluy, I. Guvency, N. Palay, and M. Yukselz, "AOA-based localization and tracking in multi-element VLC systems," in *Proc. IEEE 16th Annu. Wireless Microw. Technol. Conf. (WAMICON)*, Cocoa Beach, FL, USA, 2015, pp. 1–5.

[82] D. Zheng, K. Cui, B. Bai, G. Chen, and J. A. Farrell, "Indoor localization based on LEDs," in *Proc. IEEE Int. Conf. Control Appl. (CCA)*, Denver, CO, USA, 2011, pp. 573–578.

[83] R. G. Brown and P. Y. C. Hwang, "Introduction to random signals and applied Kalman filtering: With MATLAB exercises and solutions," in *Introduction Random Signals and Applied Kalman Filtering: With MATLAB Exercises and Solutions*, vol. 1, R. G. Brown and P. Y. C. Hwang, Eds. New York, NY, USA: Wiley, 1997.

[84] M. S. Grewal, "Kalman filtering," *Embedded Syst. Program.*, vol. 14, no. 2, pp. 90–92, 2011.

[85] S.-H. P. Won, W. W. Melek, and F. Golnaraghi, "A Kalman/particle filter-based position and orientation estimation method using a position sensor/inertial measurement unit hybrid system," *IEEE Trans. Ind. Electron.*, vol. 57, no. 5, pp. 1787–1798, May 2010.

[86] D.-J. Jwo and S.-H. Wang, "Adaptive fuzzy strong tracking extended Kalman filtering for GPS navigation," *IEEE Sensors J.*, vol. 7, no. 5, pp. 778–789, May 2007.

[87] L. Hostetler and R. Andreas, "Nonlinear Kalman filtering techniques for terrain-aided navigation," *IEEE Trans. Autom. Control*, vol. AC-28, no. 3, pp. 315–323, Mar. 1983.

[88] R. Van Der Merwe and E. A. Wan, "Sigma-point Kalman filters for integrated navigation," in *Proc. 60th Annu. Meeting Inst. Navig. (ION)*, 2004, pp. 641–654.

[89] J. L. Crassidis, "Sigma-point Kalman filtering for integrated GPS and inertial navigation," *IEEE Trans. Aerosp. Electron. Syst.*, vol. 42, no. 2, pp. 750–756, Apr. 2006.

[90] R. Van Der Merwe, A. Doucet, N. De Freitas, and E. Wan, "The unscented particle filter," in *Proc. NIPS*, Denver, CO, USA, 2000, pp. 584–590.

[91] A. Doucet and A. M. Johansen, "A tutorial on particle filtering and smoothing: Fifteen years later," *Handbook Nonlin. Filtering*, vol. 12, nos. 656–704, p. 3, Dec. 2009.

[92] D. Crisan and A. Doucet, "A survey of convergence results on particle filtering methods for practitioners," *IEEE Trans. Signal Process.*, vol. 50, no. 3, pp. 736–746, Mar. 2002.

[93] M. S. Arulampalam, S. Maskell, N. Gordon, and T. Clapp, "A tutorial on particle filters for online nonlinear/non-Gaussian Bayesian tracking," *IEEE Trans. Signal Process.*, vol. 50, no. 2, pp. 174–188, Feb. 2002.

[94] D. Ganti, W. Zhang, and M. Kavehrad, "VLC-based indoor positioning system with tracking capability using Kalman and particle filters," in *Proc. IEEE Int. Conf. Consum. Electron. (ICCE)*, Las Vegas, NV, USA, 2014, pp. 476–477.

[95] M. T. Taylor and S. Hranilovic, "Angular diversity approach to indoor positioning using visible light," in *Proc. IEEE Globecom Workshops (GC Wkshps)*, Atlanta, GA, USA, 2013, pp. 1093–1098.

[96] J. Herrnsdorf, M. J. Strain, E. Gu, R. K. Henderson, and M. D. Dawson, "Positioning and space-division multiple access enabled by structured illumination with light-emitting diodes," *J. Lightw. Technol.*, vol. 35, no. 12, pp. 2339–2345, Jun. 15, 2017.

[97] P. F. Mmbaga, J. Thompson, and H. Haas, "Performance analysis of indoor diffuse VLC MIMO channels using angular diversity detectors," *J. Lightw. Technol.*, vol. 34, no. 4, pp. 1254–1266, Feb. 15, 2016.

[98] Q. Xu, R. Zheng, and S. Hranilovic, "IDyLL: Indoor localization using inertial and light sensors on smartphones," presented at the ACM Int. Joint Conf. Pervasive Ubiquitous Comput., Osaka, Japan, 2015, pp. 307–318.

[99] H. Steendam, T. Q. Wang, and J. Armstrong, "Cramer-Rao bound for indoor visible light positioning using an aperture-based angular-diversity receiver," in *Proc. IEEE Int. Conf. Commun. (ICC)*, Kuala Lumpur, Malaysia, 2016, pp. 1–6.

[100] C. Danakis, M. Afgani, G. Povey, I. Underwood, and H. Haas, "Using a CMOS camera sensor for visible light communication," in *Proc. IEEE Globecom Workshops*, Anaheim, CA, USA, 2012, pp. 1244–1248.

[101] J. Ferrandiz-Lahuerta, D. Camps-Mur, and J. Paradells-Aspas, "A reliable asynchronous protocol for VLC communications based on the rolling shutter effect," in *Proc. IEEE Glob. Commun. Conf. (GLOBECOM)*, San Diego, CA, USA, 2015, pp. 1–6.

[102] T. Sonoda, H. Nagahara, K. Endo, Y. Sugiyama, and R.-I. Taniguchi, "High-speed imaging using CMOS image sensor with quasi pixel-wise exposure," in *Proc. IEEE Int. Conf. Comput. Photography (ICCP)*, Evanston, IL, USA, 2016, pp. 1–11.

[103] M. Li, B. H. Kim, and A. I. Mourikis, "Real-time motion tracking on a cellphone using inertial sensing and a rolling-shutter camera," in *Proc. IEEE Int. Conf. Robot. Autom. (ICRA)*, Karlsruhe, Germany, 2013, pp. 4712–4719.

[104] M. Liu *et al.*, "Towards indoor localization using visible light communication for consumer electronic devices," in *Proc. IEEE/RSJ Int. Conf. Intell. Robots Syst.*, Chicago, IL, USA, 2014, pp. 143–148.

[105] M. S. Rahman, M. M. Haque, and K.-D. Kim, "High precision indoor positioning using lighting LED and image sensor," in *Proc. 14th Int. Conf. Comput. Inf. Technol. (ICCIT)*, Dhaka, Bangladesh, 2011, pp. 309–314.

[106] M. S. Rahman, M. M. Haque, and K.-D. Kim, "Indoor positioning by LED visible light communication and image sensors," *Int. J. Elect. Comput. Eng.*, vol. 1, no. 2, p. 161, 2011.

[107] H. Huang, L. Feng, G. Ni, and A. Yang, "Indoor imaging visible light positioning with sampled sparse light source and mobile device," *Chin. Opt. Lett.*, vol. 14, no. 9, 2016, Art. no. 090602.

[108] Z. Li, A. Yang, H. Lv, L. Feng, and W. Song, "Fusion of visible light indoor positioning and inertial navigation based on particle filter," *IEEE Photon. J.*, vol. 9, no. 3, pp. 1–13, Oct. 2017.

[109] Z. Luo, W. Zhang, and G. Zhou, "Improved spring model-based collaborative indoor visible light positioning," *Opt. Rev.*, vol. 23, no. 3, pp. 479–486, 2016.

[110] S. Hyun, Y. Lee, J. Lee, M. Ju, and Y. Park, "Indoor positioning using optical camera communication & pedestrian dead reckoning," in *Proc. 7th Int. Conf. Ubiquitous Future Netw. (ICUFN)*, 2015, pp. 64–65.
[111] B. Xie *et al.*, "LIPS: A light intensity–based positioning system for indoor environments," *ACM Trans. Sen. Netw.*, vol. 12, no. 4, pp. 1–27, 2016.
[112] R. Zhang, W.-D. Zhong, D. Wu, and K. Qian, "A novel sensor fusion based indoor visible light positioning system," in *Proc. IEEE Globecom Workshops (GC Wkshps)*, Washington, DC, USA, 2016, pp. 1–6.
[113] D. Taniuchi, X. Liu, D. Nakai, and T. Maekawa, "Spring model based collaborative indoor position estimation with neighbor mobile devices," *IEEE J. Sel. Topics Signal Process.*, vol. 9, no. 2, pp. 268–277, Mar. 2015.
[114] E. Edwards and S. Hranilovic, "Indoor localization using low-complexity luminaires and ambient light sensors," in *Proc. IEEE Photon. Soc. Summer Topical Meeting Series (SUM)*, Newport Beach, CA, USA, 2016, pp. 154–155.
[115] H. S. Liu and G. Pang, "Positioning beacon system using digital camera and LEDs," *IEEE Trans. Veh. Technol.*, vol. 52, no. 2, pp. 406–419, Mar. 2003.
[116] B. Bai, G. Chen, Z. Xu, and Y. Fan, "Visible light positioning based on LED traffic light and photodiode," in *Proc. IEEE Veh. Technol. Conf. (VTC Fall)*, San Francisco, CA, USA, 2011, pp. 1–5.
[117] R. Roberts, P. Gopalakrishnan, and S. Rathi, "Visible light positioning: Automotive use case," in *Proc. IEEE Veh. Netw. Conf.*, Jersey City, NJ, USA, 2010, pp. 309–314.
[118] B. W. Kim and S.-Y. Jung, "Vehicle positioning scheme using V2V and V2I visible light communications," in *Proc. IEEE 83rd Veh. Technol. Conf. (VTC Spring)*, Nanjing, China, 2016, pp. 1–5.
[119] N. Krommenacker, Ó. C. Vásquez, M. D. Alfaro, and I. Soto, "A self-adaptive cell-ID positioning system based on visible light communications in underground mines," in *Proc. IEEE Int. Conf. Automatica (ICA-ACCA)*, Curicó, Chile, 2016, pp. 1–7.
[120] J. Bosch, N. Gracias, P. Ridao, K. Istenič, and D. Ribas, "Close-range tracking of underwater vehicles using light beacons," *Sensors*, vol. 16, no. 4, p. 429, 2016.
[121] S.-H. Yang, D.-R. Kim, H.-S. Kim, Y.-H. Son, and S.-K. Han, "Visible light based high accuracy indoor localization using the extinction ratio distributions of light signals," *Microw. Opt. Technol. Lett.*, vol. 55, no. 6, pp. 1385–1389, 2013.
[122] M. Yasir, S.-W. Ho, and B. N. Vellambi, "Indoor position tracking using multiple optical receivers," *J. Lightw. Technol.*, vol. 34, no. 4, pp. 1166–1176, Feb. 15, 2016.
[123] Y. Hou, S. Xiao, H. Zheng, and W. Hu, "Multiple access scheme based on block encoding time division multiplexing in an indoor positioning system using visible light," *IEEE/OSA J. Opt. Commun. Netw.*, vol. 7, no. 5, pp. 489–495, May 2015.
[124] J. Quan, B. Bai, S. Jin, and Y. Zhang, "Indoor positioning modeling by visible light communication and imaging," *Chin. Opt. Lett.*, vol. 12, no. 5, 2014, Art. no. 052201.
[125] R. Zhang, W.-D. Zhong, K. Qian, and D. Wu, "Image sensor based visible light positioning system with improved positioning algorithm," *IEEE Access*, vol. 5, pp. 6087–6094, 2017.
[126] H. G. Myung, J. Lim, and D. J. Goodman, "Single carrier FDMA for uplink wireless transmission," *IEEE Veh. Technol. Mag.*, vol. 1, no. 3, pp. 30–38, Sep. 2006.
[127] L. Yin, W. O. Popoola, X. Wu, and H. Haas, "Performance evaluation of non-orthogonal multiple access in visible light communication," *IEEE Trans. Commun.*, vol. 64, no. 12, pp. 5162–5175, Dec. 2016.
[128] T. S. Rappaport *et al.*, "Millimeter wave mobile communications for 5G cellular: It will work!" *IEEE Access*, vol. 1, pp. 335–349, 2013.
[129] *Wireless LAN at 60 GHz—IEEE 802.11ad Explained: Application Note*, Agilent Technol., Santa Clara, CA, USA, 2013.
[130] Samsung. (Oct. 13, 2014). *Samsung Electronics' 60GHz Wi-Fi Technology Accelerates Data Transmission by Five Times*. [Online]. Available: http://www.samsung.com/uk/news/local/samsung-electronics-60ghz-wi-fi-technology-accelerates-data-transmission-by-five-times
[131] P. Cao and J. S. Thompson, "The role of analog beamwidth in spectral efficiency of millimeter wave ad hoc networks," in *Proc. 1st Int. Conf. Smart Grid Inspired Future Technol. (SmartGIFT)*, 2017, pp. 98–104.
[132] P. Cao and J. S. Thompson, "Practical multi-user transmission design in millimeter wave cellular networks: Is the joint SDMA-TDMA technique the answer?" in *Proc. IEEE 17th Int. Workshop Signal Process. Adv. Wireless Commun. (SPAWC)*, Edinburgh, U.K., 2016, pp. 1–5.
[133] F. Lemic *et al.*, "Localization as a feature of mmWave communication," in *Proc. IEEE Int. Conf. Wireless Commun. Mobile Comput.*, Paphos, Cyprus, 2016, pp. 1033–1038.
[134] H. Deng and A. Sayeed, "Mm-wave MIMO channel modeling and user localization using sparse beamspace signatures," in *Proc. IEEE 15th Int. Workshop Signal Process. Adv. Wireless Commun. (SPAWC)*, Toronto, ON, Canada, 2014, pp. 130–134.

Yuan Zhuang (M'16) received the bachelor's degree in information engineering and the master's degree in microelectronics and solid state electronics from Southeast University, Nanjing, China, in 2008 and 2011, respectively, and the Ph.D. degree in geomatics engineering from the University of Calgary, Canada, in 2015. Since 2015, he has been a Lead Scientist with Bluvision Inc., Fort Lauderdale, FL, USA. He was a Baseband Engineer with CSR Technology, Shanghai Company Ltd., Shanghai, China and an Algorithm Designer with Trusted Positioning Inc., Calgary, Canada. His current research interests include real-time location system, personal navigation system, wireless positioning, multisensors integration, Internet of Things, and machine learning for navigation applications. He has co-authored over 30 academic papers and 11 patents. He was a recipient of over ten academic awards, such as, the Best Paper Award for Young Scientists from China Satellite Navigation Conference, the Best Paper Award from the 28th International Technical Meeting of The Satellite Division of the Institute of Navigation (ION GNSS+ 2015), the Winner of the 5th EvAAL-ETRI Competition, Track 1: Smartphone based positioning, the 2015 Outstanding Reviewer for IEEE TRANSACTIONS ON INSTRUMENTATION AND MEASUREMENT, and the Mitacs Accelerate Award from Mitacs—Inspiring innovation in Canada. He is a reviewer of several IEEE journals and the Lead Guest Editor for the upcoming special issue "Towards Positioning, Navigation, and Location Based Services for Internet of Things" of the IEEE INTERNET OF THINGS JOURNAL.

Luchi Hua received the B.S. degree from the Harbin Institute of Technology, Harbin, China, in 2014. He is currently pursuing the master's degree in integrated circuit engineering with Southeast University, Nanjing, China. His current research interests including wireless communication and its applications to the field of indoor positioning.

Longning Qi was born in Zhejiang, China, in 1979. He received the B.S. degree in communication engineering, and the M.S. and Ph.D. degrees in microelectronics and solid-state electronics from Southeast University, Jiangsu, China, in 2001, 2003, and 2008, respectively, where he has been with National ASIC System Engineering Research Center since 2008. His current research interests include low power design, GNSS tracking, sensor fusion, and indoor location.

Jun Yang received the bachelor's, master's, and Ph.D. degrees from Southeast University in 1999, 2001, and 2004, respectively. He is a Professor in National ASIC Center, Southeast University, Nanjing, China. His research interests include near threshold circuit design and ultra-low power indoor/outdoor position algorithm and chips. He owned three U.S. patents, one EU patent, over 30 Chinese patents, and co-authored over 30 academic papers. He supervised and graduated over 30 master's and Ph.D. students. He was a recipient of several national awards including the State Science and Technology Awards.

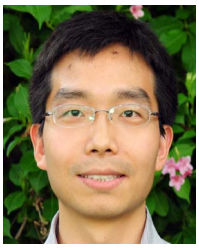

Pan Cao (S'12–M'15) received the B.Eng. degree in mechano-electronic engineering and the M.Eng. degree in information and signal processing from Xidian University, Xi'an, China, in 2008 and 2011, respectively, and the Dr.-Ing (Ph.D.) degree in electrical engineering from TU Dresden, Germany, in 2015. From 2015 to 2017, he was a Post-Doctoral Research Associate with the Institutes for Digital Communications, University of Edinburgh, U.K., supported by the EPSRC project SERAN (Seamless and Efficient Wireless Access for Future Radio Networks). He was also a Visiting Post-Doctoral Research Associate with Princeton University during the first three months of 2017. Since 2017, he has been a Senior Lecturer with the School of Engineering and Technology, University of Hertfordshire, U.K. His current research interests include millimeter-wave communication, signal processing for radar and communications, and nonconvex optimization. He was a recipient of the Best Student Paper Award of the 13th IEEE International Workshop on Signal Processing Advances in Wireless Communications, Cesme, Turkey, in 2012 and the Qualcomm Innovation Fellowship Award in 2013.

Yue Cao (M'16) received the Ph.D. degree from the Institute for Communication Systems (formerly Centre for Communication Systems Research), University of Surrey, Guildford, U.K., in 2013, and continued his work further as a Research Fellow. In 2016, he was a Lecturer, and in 2017, a Senior Lecturer with the Department of Computer and Information Sciences, Northumbria University, Newcastle upon Tyne, U.K. His research interests focus on delay/disruption tolerant networks, E-mobility, autonomous valet parking, and QoS/QoE in 5G. He is a reviewer of several IEEE journals and an Associate Editor of the IEEE ACCESS.

Yongpeng Wu (S'08–M'13–SM'17) received the B.S. degree in telecommunication engineering from Wuhan University, Wuhan, China, in 2007, and the Ph.D. degree in communication and signal processing from the National Mobile Communications Research Laboratory, Southeast University, Nanjing, China, in 2013. He is currently a Tenure-Track Associate Professor with the Department of Electronic Engineering, Shanghai Jiao Tong University, China. He was a Senior Research Fellow with the Institute for Communications Engineering, Technical University of Munich, Germany, and the Humboldt Research Fellow and the Senior Research Fellow with the Institute for Digital Communications, University Erlangen-Nuremberg, Germany. During his doctoral studies, he conducted cooperative research with the Department of Electrical Engineering, Missouri University of Science and Technology, USA. His research interests include massive MIMO/MIMO systems, physical layer security, signal processing for wireless communications, and multivariate statistical theory. He was a recipient of the IEEE Student Travel Grants for IEEE International Conference on Communications (ICC) 2010, the Alexander von Humboldt Fellowship in 2014, the Travel Grants for IEEE Communication Theory Workshop 2016, and the Excellent Doctoral Thesis Awards of China Communications Society 2016. He was an Exemplary Reviewer of the IEEE TRANSACTIONS ON COMMUNICATIONS in 2015 and 2016. He is the Lead Guest Editor for the upcoming special issue "Physical Layer Security for 5G Wireless Networks" of the IEEE JOURNAL ON SELECTED AREAS IN COMMUNICATIONS. He is currently an Editor of the IEEE ACCESS and the IEEE COMMUNICATIONS LETTERS. He has been a TPC member of various conferences, including Globecom, ICC, VTC, and PIMRC.

John Thompson (M'94–SM'13–F'16) is currently the Personal Chair in Signal Processing and Communications with the University of Edinburgh, U.K. His main research interests are in wireless communications, sensor signal processing and energy efficient communications networks, and smart grids. He has published around 300 papers in these topics. He was a recipient of the Highly Cited Researcher Award from Thomson Reuters in 2015 and 2016. He also currently leads the European Marie Curie Training Network ADVANTAGE, which trains 13 Ph.D. students in smart grids. He was a Distinguished Lecturer on green topics for ComSoc in 2014 and 2015. He is also currently an Editor of the Green Series of *IEEE Communications Magazine* and an Associate Editor for the IEEE TRANSACTIONS ON GREEN COMMUNICATIONS AND NETWORKS.

Harald Haas received the Ph.D. degree from the University of Edinburgh in 2001. He currently holds the Chair of Mobile Communications with the University of Edinburgh, and is a Co-Founder and the Chief Scientific Officer of pureLiFi Ltd as well as the Director of the LiFi Research and Development Center, University of Edinburgh. His main research interests are in optical wireless communications, hybrid optical wireless and RF communications, spatial modulation, and interference coordination in wireless networks. He first introduced and coined spatial modulation and LiFi. LiFi was listed among the 50 best inventions in *TIME Magazine* 2011. He was an Invited Speaker at TED Global 2011, and his talk "Wireless Data from Every Light Bulb" has been watched online over 2.4 million times. He gave a second TED Global lecture in 2015 on the use of solar cells as LiFi data detectors and energy harvesters, which has been viewed online over 1.8 million times. He holds 31 patents and has over 30 pending patent applications. He has published 400 conference and journal papers including a paper in *Science*. He has co-authored a book entitled *Principles of LED Light Communications Towards Networked Li-Fi* (Cambridge University Press, 2015). He is an Editor of the IEEE TRANSACTIONS ON COMMUNICATIONS and IEEE JOURNAL OF LIGHTWAVE TECHNOLOGIES. He was a recipient of the Prestigious Established Career Fellowship from the EPSRC (Engineering and Physical Sciences Research Council) within Information and Communications Technology in U.K, in 2012 and the Outstanding Achievement Award from the International Solid State Lighting Alliance in 2016. He was co-recipient of recent best paper awards at VTC-Fall, 2013, VTC-Spring 2015, ICC 2016, and ICC 2017, the EURASIP Best Paper Award for the *Journal on Wireless Communications and Networking* in 2015, and the Jack Neubauer Memorial Award of the IEEE Vehicular Technology Society. In 2014, he was selected by EPSRC as one of ten Recognising Inspirational Scientists and Engineers Leaders in U.K. He was Elected a Fellow of the Royal Society of Edinburgh in 2017.